



# Rhodolith Physiology Across the Atlantic: Towards a Better Mechanistic Understanding of Intra- and Interspecific Differences

## OPEN ACCESS

### Edited by:

Bernardo Antonio Perez Da Gama,  
Fluminense Federal University, Brazil

### Reviewed by:

Christopher Edward Cornwall,  
Victoria University of Wellington, New Zealand

John Albert Raven,  
University of Dundee, United Kingdom

### \*Correspondence:

Nadine Schubert  
nadine\_schubert@hotmail.com

### †Present Address:

Vinicius W. Salazar,  
Melbourne Integrative Genomics, The  
University of Melbourne, Parkville, VIC,  
Australia

‡These authors have contributed  
equally to this work

### Specialty section:

This article was submitted to  
Marine Ecosystem Ecology,  
a section of the journal  
Frontiers in Marine Science

**Received:** 16 April 2022

**Accepted:** 31 May 2022

**Published:** 24 June 2022

### Citation:

Schubert N, Peña V, Salazar VW,  
Horta PA, Neves P, Ribeiro C, Otero-  
Ferrer F, Tuya F, Espino F,  
Schoenrock K, Hofmann LC, Le Gall L,  
Santos R and Silva J (2022) Rhodolith  
Physiology Across the Atlantic:  
Towards a Better Mechanistic  
Understanding of Intra- and  
Interspecific Differences.  
Front. Mar. Sci. 9:921639.  
doi: 10.3389/fmars.2022.921639

Nadine Schubert<sup>1\*</sup>, Viviana Peña<sup>2‡</sup>, Vinicius W. Salazar<sup>3†‡</sup>, Paulo A. Horta<sup>3‡</sup>,  
Pedro Neves<sup>1,4‡</sup>, Cláudia Ribeiro<sup>1,4,5‡</sup>, Francisco Otero-Ferrer<sup>6,7‡</sup>, Fernando Tuya<sup>6‡</sup>,  
Fernando Espino<sup>6‡</sup>, Kathryn Schoenrock<sup>8‡</sup>, Laurie C. Hofmann<sup>9</sup>, Line Le Gall<sup>10</sup>,  
Rui Santos<sup>1</sup> and João Silva<sup>1</sup>

<sup>1</sup> Centre of Marine Sciences (CCMAR), University of Algarve, Faro, Portugal, <sup>2</sup> BioCost Research Group, Departamento de Biología, Facultad de Ciencias, Universidad de Coruña, A Coruña, Spain, <sup>3</sup> Laboratório de Fisiologia, Departamento de Botânica, Centro de Ciências Biológicas, Universidade Federal de Santa Catarina, Florianópolis, Brazil, <sup>4</sup> Observatório Oceânico da Madeira, Agência Regional para o Desenvolvimento da Investigação, Tecnologia e Inovação (OOM/ARDITI), Edifício Madeira Tecnopolo, Funchal, Portugal, <sup>5</sup> Instituto das Florestas e Conservação da Natureza (IFCN), IP-RAM, Madeira, Funchal, Portugal, <sup>6</sup> Grupo en Biodiversidad y Conservación (IU-ECOQUA), Universidad de Las Palmas de Gran Canaria, Telde, Spain, <sup>7</sup> Asociación Biodiversidad Atlántica y Sostenibilidad (ABAS), Telde, Spain, <sup>8</sup> Department of Zoology, School of Natural Sciences, The Ryan Institute for Environmental, Marine and Energy Research, National University of Ireland Galway, Galway, Ireland, <sup>9</sup> Marine Aquaculture Group, Alfred Wegener Institute Helmholtz Center for Polar and Marine Research, Bremerhaven, Germany, <sup>10</sup> Institut de Systématique, Évolution, Biodiversité (ISYEB), Muséum National d'Histoire Naturelle, CNRS, Sorbonne Université, EPHE, Université des Antilles, Paris, France

Coralline algae are important components in a large variety of ecosystems. Among them, rhodoliths are a group of free-living coralline red algae that cover extensive coastal areas, from tropical to polar regions. In contrast to other ecosystem engineers, limited research efforts preclude our understanding of their physiology, underlying mechanisms, drivers and potential differences related to species under varying environments. In this study, we investigated the photosynthetic and calcification mechanisms of six Atlantic rhodolith species from different latitudes, as well as intra-specific differences in one species from four locations. Laboratory incubations under varying light levels provided simultaneous photosynthesis- and calcification-irradiance curves, allowing the assessment of inter- and intra-specific differences on the coupling between these two processes. Stable isotope analysis and specific inhibitor experiments were performed to characterize and compare carbon-concentrating mechanisms (CCMs), as well as the involvement of specific ion-transporters for calcification. Our findings showed significant differences in rhodolith physiological mechanisms that were partially driven by local environmental conditions (light, temperature). High variability was found in the coupling between photosynthesis and calcification, in CCM-strategies, and in the importance of specific ion transporters and enzymes involved in calcification. While calcification was strongly correlated with photosynthesis in all species, the strength of this link was species-specific. Calcification was also found to be reliant on photosynthesis- and light-independent processes. The latter showed a high plasticity in their expression among species, also influenced by the

local environment. Overall, our findings demonstrate that (1) rhodolith calcification is a biologically-controlled process and (2) the mechanisms associated with photosynthesis and calcification display a large variability among species, suggesting potential differences not only in their individual, but also community responses to environmental changes, such as climate change.

**Keywords:** calcification mechanism, carbon-concentrating mechanism (CCM), coralline algae (maërl), photosynthesis-calcification relationship, rhodolith beds

## INTRODUCTION

Free-living coralline algae are known to form major marine carbonate-producing ecosystems, so-called rhodolith beds that provide habitat for a high diversity of fauna and flora (Riosmena-Rodriguez et al., 2017). These ecosystems occupy extensive areas around the world, from polar to tropical regions (Foster, 2001; Riosmena-Rodriguez et al., 2017), and the increasing number of recent discoveries (e.g., Harvey et al., 2017; Rebelo et al., 2018; Sreeraj et al., 2018; Bracchi et al., 2019; Jeong et al., 2019; Adams et al., 2020; Otero-Ferrer et al., 2020; Ribeiro and Neves, 2020; Neves et al., 2021; Ward et al., 2021), and global distributional models (Fragkopoulou et al., 2021; Rebelo et al., 2021), suggest that rhodolith beds may have an even wider distribution than anticipated, mainly shaped by temperature, light, pH, nutrients and water current velocity (Carvalho et al., 2020; Fragkopoulou et al., 2021; Sissini et al., 2021).

Despite their worldwide distribution and the acknowledged ecological services that rhodolith beds provide in coastal regions (Riosmena-Rodriguez et al., 2017), knowledge regarding organism- and community-level physiological performance and productivity is still scarce and regionally focused, e.g. in Europe (Figure 1A). At the community level, a few studies have been performed on temperate European rhodolith beds, to determine rhodolith-bed productivity or *in situ* effects of ocean acidification (Martin et al., 2005; Martin et al., 2007a; Attard et al., 2015; Burdett et al., 2018). Similarly, at the organismal level, our understanding of rhodolith physiological mechanisms and species-specific differences is still majorly lacking. A recent analysis identified a total of 106 rhodolith-forming species worldwide (Rebelo et al., 2021), though at a global scale, scattered physiological information is currently available for 15 species only (Figure 1A).

Overall, coralline algal species have been shown to express a high variability regarding their physiological performance under similar environmental conditions (e.g., Chisholm, 2000; Chisholm, 2003; Vásquez-Elizondo and Enríquez, 2016; Qui-Minet et al., 2021; Schubert et al., 2021a), which suggest differences in physiological mechanisms and/or the extent to which they are expressed. This assumption is supported by recent studies that showed a high plasticity in inorganic carbon uptake strategies for photosynthesis (Hofmann and Heesch, 2018; Zweng et al., 2018; Bergstrom et al., 2020). Also, comparisons among different species, from the same habitat, suggest a variability in the strength of the coupling between photosynthesis and calcification (Vásquez-Elizondo and

Enríquez, 2016; Qui-Minet et al., 2021). The direct relationship between these processes was demonstrated early on (Digby, 1977; Pentecost, 1978; Borowitzka, 1981; Borowitzka, 1987) and is supported by recent studies (e.g., Martin et al., 2013; Vásquez-Elizondo and Enríquez, 2016; Sordo et al., 2019), which showed a decline in calcification upon inhibition of photosynthesis (Hofmann et al., 2016; McNicholl et al., 2019). This link has been related to an elevation of the pH at the calcification site due to photosynthetic activity. Considering differences in species' metabolic rates (Chisholm, 2000; Chisholm, 2003; Vásquez-Elizondo and Enríquez, 2016; Qui-Minet et al., 2021) and morphological traits, which affect pH conditions in the diffusive boundary layer (DBL; Cornwall et al., 2017; Schubert et al., 2021a) that are positively correlated with the pH of the calcifying fluid ( $\text{pH}_{\text{cf}}$ ; Comeau et al., 2019a), it can be assumed that its strength varies among species. Furthermore, coralline  $\text{CaCO}_3$  precipitation in the dark, with lower and highly variable rates among species (e.g., Chisholm, 2000; Vásquez-Elizondo and Enríquez, 2016; Qui-Minet et al., 2021; Schubert et al., 2021a), and when photosynthesis is inhibited (Hofmann et al., 2016; Hofmann et al., 2018) suggests that calcification is partially independent from photosynthesis. Hence, the relationship between the two processes might be species-specific.

Coralline algal calcification occurs within the cell walls, up to three cell layers deep (primary calcification), while secondary calcification can occur as interfilament precipitation between cells and conceptacle in-filling (Borowitzka, 1987; Adey et al., 2013). The physiological process of calcification in coralline algae is still poorly understood, though over the last decade several conceptual models have been proposed. It has been suggested that calcification is a biologically induced, rather than a controlled process, associated with cell wall organic-matrix-induced mineralization (Nash et al., 2019). However, mechanistic studies and derived models suggest that coralline algae exert some control over the calcification process, by promoting favorable conditions for  $\text{CaCO}_3$  precipitation through photosynthesis and active dissolved inorganic carbon (DIC) and ion transport pathways (Comeau et al., 2013; Koch et al., 2013; Hofmann et al., 2016; Cornwall et al., 2017; McNicholl et al., 2019). Recent studies showed that the extent of photosynthesis-promoted increase of pH in the DBL ( $\text{pH}_{\text{DBL}}$ ) is species-specific and influenced by external seawater pH, but also by species' morphology, due to its strong influence on DBL thickness (Cornwall et al., 2017; Hofmann et al., 2018; Schubert et al., 2021a). Further evidence suggests that it is coupled to the activity of the external carbonic anhydrase ( $\text{CA}_{\text{ext}}$ ) and active

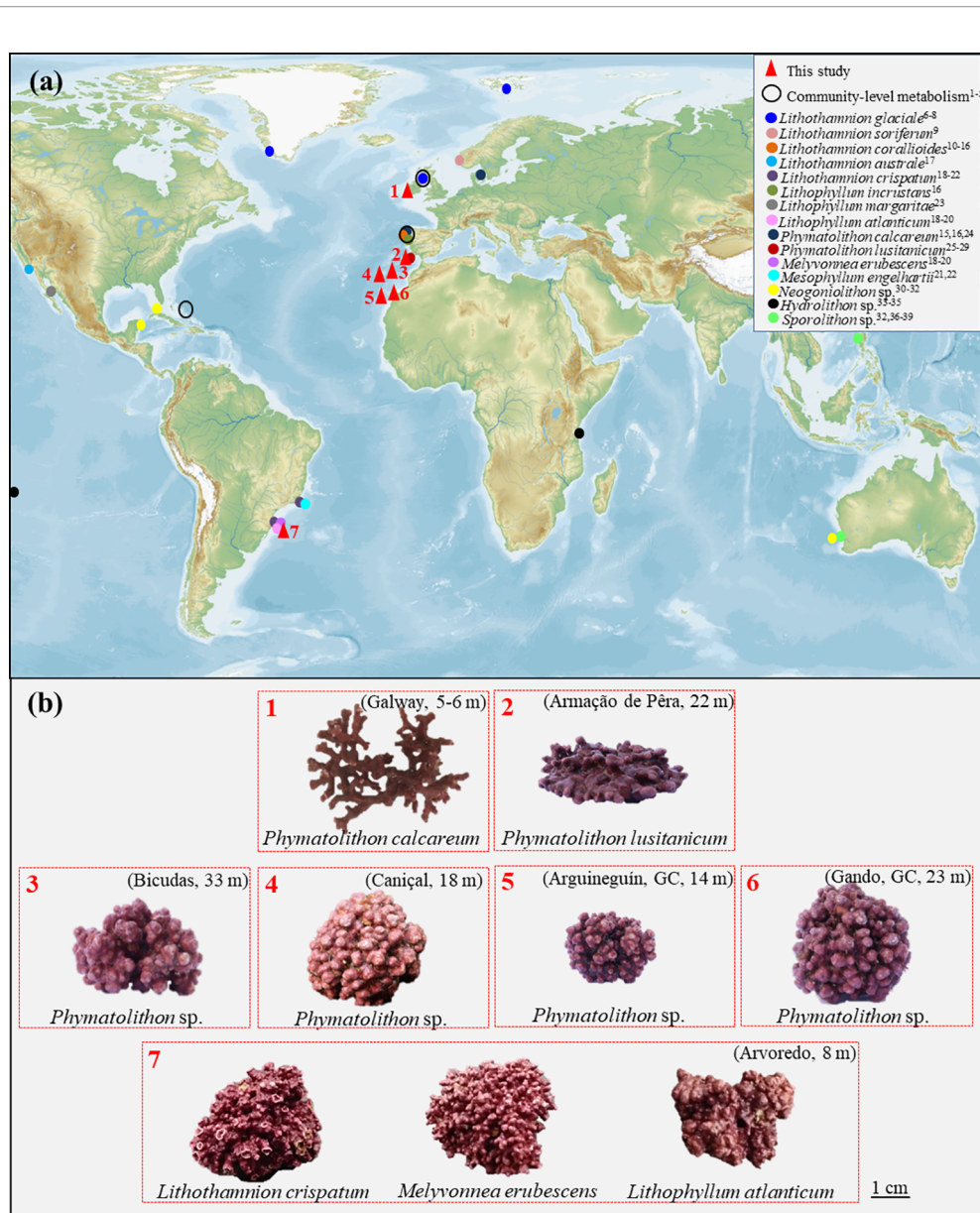


**FIGURE 1 | (A)** Overview of rhodolith species and locations for which primary production and/or calcification rates have been reported. Sampling locations of rhodolith species studied in this work are indicated by red triangles (1- Galway, Ireland; 2- Armação de Pêra, South Portugal; 3- Bicudas, Porto Santo Island, Portugal; 4- Caniçal, Madeira Island, Portugal; 5- Arguineguín, Gran Canaria, Spain; 6- Gando, Gran Canaria, Spain; 7- Arvoredo, South Brazil). **(B)** Studied rhodolith species and their respective sampling location and depth (in parenthesis). Map was downloaded from Mapswire (<https://mapswire.com/>). (<sup>1</sup>Martin et al., 2005; <sup>2</sup>Martin et al., 2007a; Martin et al., 2007b; <sup>3</sup>Attard et al., 2015; <sup>4</sup>Burdett et al., 2018; <sup>5</sup>Little et al., 1991; <sup>6</sup>Büdenbender et al., 2011; <sup>7</sup>Kamenos et al., 2013; <sup>8</sup>Schoenrock et al., 2018; <sup>9</sup>Legrand et al., 2021; <sup>10</sup>Martin et al., 2006; <sup>11</sup>Noisette et al., 2013a; <sup>12</sup>Noisette et al., 2013b; <sup>13</sup>Legrand et al., 2017; <sup>14</sup>Legrand et al., 2019; <sup>15</sup>Qui-Minet et al., 2019; <sup>16</sup>Qui-Minet et al., 2021; <sup>17</sup>Kim et al., 2020; <sup>18</sup>Schubert et al., 2019; <sup>19</sup>Carvalho et al., 2020; <sup>20</sup>Schubert et al., 2021a; <sup>21</sup>Reynier et al., 2015; <sup>22</sup>Figueiredo et al., 2012; <sup>23</sup>Steller et al., 2007; <sup>24</sup>King and Schramm, 1982; <sup>25</sup>Sordo et al., 2016; <sup>26</sup>Sordo et al., 2018; <sup>27</sup>Sordo et al., 2019; <sup>28</sup>Sordo et al., 2020; <sup>29</sup>Schubert et al., 2021b; <sup>30</sup>Zweng et al., 2018; <sup>31</sup>Vásquez-Elizondo and Enríquez, 2016; <sup>32</sup>Cornwall et al., 2017; <sup>33</sup>Semesi et al., 2009; <sup>34</sup>Payri, 1997; <sup>35</sup>Cornwall et al., 2018; <sup>36</sup>Comeau et al., 2018; <sup>37</sup>Comeau et al., 2019a; <sup>38</sup>Comeau et al., 2019b; <sup>39</sup>Narvarte et al., 2020).

influx and efflux of protons (Hofmann et al., 2016). In fact, it is generally assumed that an active proton transport exists in the form of an antiport, symport and/or a proton pump, likely involving  $\text{HCO}_3^-/\text{H}^+$  and/or  $\text{OH}^-/\text{H}^+$  symport and/or a  $\text{Ca}^{2+}$ -driven ATPase (Okazaki, 1977; Borowitzka, 1987; McConnaughey and Falk, 1991; Mori et al., 1996; Comeau et al., 2013; Koch et al., 2013; Hofmann

et al., 2016; Cornwall et al., 2017; Hofmann et al., 2018; McNicholl et al., 2019). In addition, microsensor studies demonstrated (a) the presence of a light-induced, but photosynthesis-independent mechanism that contributes to the pH dynamics at the algal thallus surface (Hofmann et al., 2016; Hofmann et al., 2018; McNicholl et al., 2019), and (b) that an elevated thallus surface

pH in darkness in an Arctic rhodolith may sustain calcification under these conditions (Hofmann et al., 2018). Finally, Comeau et al. (2019a) demonstrated a linear relationship between the pH gradient in the DBL and the  $\text{pH}_{\text{cF}}$ , which suggests that the elevation of the  $\text{pH}_{\text{DBL}}$  favors the export of protons from the calcification site by reducing the proton gradient between the calcifying fluid and the bulk seawater.

Reviewing available information for rhodoliths, it becomes evident that only a few studies have focused on a general physiological characterization, including information on specific rates of photosynthesis and/or calcification, productivity estimates, seasonal variation in physiological rates and/or a physiological comparison among species (Littler et al., 1991; Payri, 1997; Martin et al., 2006; Martin et al., 2007a; Martin et al., 2007b; Sordo et al., 2020; Qui-Minet et al., 2021; Schubert et al., 2021a). Even less information is available regarding the mechanisms driving rhodolith photosynthesis and calcification (Cornwall et al., 2017; Hofmann and Heesch, 2018; Hofmann et al., 2018; Zweng et al., 2018). Essentially, most physiological data derive from studies that assessed the effects of climate change-related and other environmental factors on rhodolith performance (King and Schramm, 1982; Steller et al., 2007; Semesi et al., 2009; Büdenbender et al., 2011; Kamenos et al., 2013; Noisette et al., 2013a; Noisette et al., 2013b; Sordo et al., 2016; Vásquez-Elizondo and Enríquez, 2016; Cornwall et al., 2017; Legrand et al., 2017; Schoenrock et al., 2018; Sordo et al., 2018; Zweng et al., 2018; Legrand et al., 2019; Sordo et al., 2019; Comeau et al., 2019a; Comeau et al., 2019b; Qui-Minet et al., 2019; Schubert et al., 2019; Carvalho et al., 2020; Kim et al., 2020; Legrand et al., 2021; Schubert et al., 2021b). These studies show that rhodoliths express a wide array of responses to

environmental changes (see also Martin and Hall-Spencer, 2017), suggesting a high variability in the mechanisms related to photosynthesis and calcification. Thus, the goal of this study was to advance our knowledge regarding these mechanisms and to identify potential species-specific differences, which could explain their variable responses and would allow identifying potential patterns. For this purpose, a general physiological characterization and comparison of rhodolith-bed forming species was performed, at the inter- and intra-specific level, specifically focusing on the mechanistic coupling between photosynthesis and calcification and potential species-specific and environmentally driven variability. Additionally, inorganic carbon uptake pathways for photosynthesis and calcification, as well as the importance of ion-transporters for these processes were compared among species.

## MATERIALS AND METHODS

### Study Locations and Sample Collections

Individuals of the predominant rhodolith species from rhodolith beds in Europe, off the coast of northwestern Africa and Brazil were collected by SCUBA diving (Figure 1) and kept under laboratory conditions during the time required for the measurements (for details see **Supplementary Material**). Samplings were undertaken during the respective warm seasons (early to late summer, 2017-2021), at depths between 5 and 33 m (Table 1). Also, light attenuation profiles in the water column were obtained ( $n=5-6$  per location), using an underwater quantum sensor (LI-192, LI-COR Environmental, USA), attached to a LI-250A Light Meter (LI-COR Environmental,

**TABLE 1** | Overview of the studied species, the locations they were collected and the respective depths and environmental conditions at the time of collection.

Species	Location	Coordinates	Depth (m)	$K_d$ ( $\text{m}^{-1}$ )	Light availability (% of surface irradiance)	Temperature ( $^{\circ}\text{C}$ )	Sampling period
<b>Cold-temperate</b>							
<i>Phymatolithon calcareum</i>	Galway, Ireland	53°18'54"N, 09°51'50"W	5.5	0.454 ± 0.15	8	16	Aug 2021
<b>Warm-temperate</b>							
<i>Phymatolithon lusitanicum</i>	Armação de Pera, South Portugal	37°06'09"N, 08°21'25"W	22	0.165 (0.09-0.240)*	3 (0.5-14)	17	Jul 2019
<i>Phymatolithon</i> sp.	Bicudas, Porto Santo Island, Portugal	33°03'37"N, 16°20'03"W	33	0.128 ± 0.01	1.5	20	Jun 2019
<i>Phymatolithon</i> sp.	Caniçal, Madeira Island, Portugal	32°44'27"N, 16°42'42"W	18	0.114 ± 0.02	13	21	Jun 2019
<b>Subtropical</b>							
<i>Phymatolithon</i> sp.	Gando, Gran Canaria, Spain	27°55'54"N, 15°21'11"W	23	0.114 ± 0.01	7	23	Oct 2019
<i>Phymatolithon</i> sp.	Arguineguín, Gran Canaria, Spain	27°45'26"N, 15°41'01"W	14	0.114 ± 0.01	20	23	Oct 2019
<i>Lithophyllum atlanticum</i>	Arvoredo, South Brazil	27°16'26"S, 48°22'1"W	8	0.194 (0.07-0.460)**	21 (3-54)	24	Dez 2017
<i>Melyvonnea erubescens</i>	Arvoredo, South Brazil	27°16'26"S, 48°22'1"W	8	0.194 (0.07-0.460)**	21 (3-54)	24	Dez 2017
<i>Lithothamnion crispatum</i>	Arvoredo, South Brazil	27°16'26"S, 48°22'1"W	8	0.194 (0.07-0.460)**	21 (3-54)	24	Dez 2017

Table Legend: Data for  $K_d$  represent mean ± SD ( $n=5-6$ ). Some locations experience strong fluctuations in  $K_d$  (min-max) due to (\*) fast inversions between up- and downwelling conditions (see Schubert et al., 2021b) and (\*\*) influence of wind-driven currents (summer  $K_d$  values from MAAE (2017).

USA), to calculate light attenuation coefficients ( $K_d$ ) for the different locations.

## Species Identification

Species were identified based on previous molecular identification of specimens collected at the sampling locations and diagnostic morphological characters, including: *Lithothamnion crispatum* Hauck (Farias et al., 2010), *Melyvonnea erubescens* (Foslie) Athanasiadis & D.L. Ballantine (Sissini et al., 2014), *Lithophyllum atlanticum* Vieira-Pinto, M.C. Oliveira & P.A. Horta (Vieira-Pinto et al., 2014), *Phymatolithon* sp. (Madeira and Porto Santo Islands; Neves et al., 2021), and *Phymatolithon lusitanicum* V. Peña (Carro et al., 2014; Pardo et al., 2014; Peña et al., 2015a).

Specimens collected in Gran Canaria (the Canary Islands) were morphologically similar to the rhodolith species *Phymatolithon* sp., collected in nearby Madeira and Porto Santo Islands (Neves et al., 2021). To confirm their conspecificity, their identification was done using molecular tools. DNA was extracted from a selection of eight specimens from two locations (six from Arguineguín, and two from Gando), using a E.Z.N.A.<sup>®</sup> Tissue DNA Kit (Omega Bio-tek, United States) and following the manufacturer protocol. The *psbA* locus was amplified using primer pairs: *psbA-F1/psbA-R2* (Yoon et al., 2002) and the thermal profile for the PCR reaction followed Peña et al. (2015b). The PCR product was purified and sequenced by the SAI-UBM department of the University of Coruña, Spain. Sequences were assembled with the assistance of CodonCode Aligner<sup>®</sup> (CodonCode Corporation, USA), adjusted by eye using SeaView version 4 (Gouy et al., 2010), and submitted to the Barcode of Life Data Systems (BOLD, Ratnasingham and Hebert, 2007) and GenBank. Estimates of genetic distance (uncorrected p-distances) between the eight *psbA* sequences generated in the present study and 29 publicly available sequences of the rhodolith species *Phymatolithon* sp. from the Madeira archipelago were calculated in MEGA v. 6 (Tamura et al., 2013). The low pairwise sequence divergence found between both regions (<0.6%, 0–5 bp difference) supported conspecificity of rhodolith collections and therefore, the identification of the Canary Islands rhodoliths as *Phymatolithon* sp.

Similarly, the identification of *Phymatolithon calcareum* (Pallas) Adey & McKibbin from Ireland was confirmed using molecular tools. The DNA of five specimens, collected in the Irish locality of Ardeast (**Table 1**), was extracted using a NucleoSpin<sup>®</sup> 96 Tissue kit (Macherey-Nagel, GmbH and Co. KG, Germany). The mitochondrial COI-5P fragment was PCR-amplified using the primer pair *GazF1* and *GazR1* (Saunders, 2005). The thermal profile for amplification and PCR reaction was as described above and the PCR products were purified and sequenced at the Muséum National d'Histoire Naturelle y Eurofins (Eurofins Scientific, Nantes, France). Sequences were assembled and analyzed as described above. The estimates of genetic distance (uncorrected p-distances) between the four COI-5P sequences, obtained from our collection and 96 publicly available sequences of *P. calcareum*, mainly from

Atlantic European coasts (Pardo et al., 2014), were calculated in MEGA v. 6 (Tamura et al., 2013). The low pairwise sequence divergence found (<0.7%, 0–5 bp difference) supported the identification of *P. calcareum*.

## Photosynthesis- and Calcification-Irradiance Curves

Rhodolith individuals from each site (n=5 per species and location) were incubated at their respective temperature, recorded during sample collection (**Table 1**), with filtered seawater (0.45  $\mu\text{m}$ ) in sealed custom-made plexiglass chambers (V=150 mL) with internal circulation provided by a magnetic stirrer. After an initial incubation in darkness to determine dark respiration rates ( $R_D$ ), rhodoliths were exposed to a series of increasing light intensities and, subsequently, they were again incubated in darkness to determine post-illumination or light respiration rates ( $R_L$ ).

The incubation time at each light intensity varied between 0.5 h, for the subtropical Brazilian species, to 1 h for the other species; this was based on previous incubations, testing different incubation times, to assure a high enough signal-to-noise ratio for measuring oxygen concentration and alkalinity. At the beginning and end of each incubation, the oxygen concentration was measured with an oxygen meter (Fibox 4, PreSens, Germany) and water samples were taken, poisoned with  $\text{HgCl}_2$  and stored in borosilicate tubes (two tubes per incubation chamber, V=25 mL each) for later estimation of calcification rates. Afterwards, the rhodoliths were dried (48 h at 60°C) and their surface area was determined by the wax-dipping method (Schubert et al., 2021a), to normalize metabolic and calcification rates and calculate surface area to dry weight ratios (SA/DW).

Gross photosynthetic rates (GP) were calculated by adding respiration rates (average of  $R_D$  and  $R_L$ ) to the measured net photosynthetic rates (NP). The photosynthetic quantum efficiency ( $\alpha$ ) was estimated from the initial slope of the light response curve, by linear least-squares regression. Irradiance of compensation ( $E_c$ ) was calculated from the ratio  $R_D/\alpha$ , and the saturation irradiance ( $E_k$ ) from the ratio  $P_{\text{max}}/\alpha$ . The maximum photosynthetic rates ( $NP_{\text{max}}$  and  $GP_{\text{max}}$ ) were obtained from the average of the maximum values above saturating irradiance. Calcification rates of the rhodolith species were determined from alkalinity measurements of seawater samples before and after each incubation, using the alkalinity anomaly principle, based on the ratio of two equivalents of total alkalinity per each mole of  $\text{CaCO}_3$  precipitation (Smith and Kinsey, 1978). For alkalinity (TA) measurements, duplicate analyses of each sample were performed, using the Gran titration method (Hansson and Jagner, 1973; Bradshaw et al., 1981). The samples were titrated with HCl 0.1 M, using an automated titration system (Titroline 7000, SI Analytics, Mainz, Germany), coupled to an autosampler (TW alpha plus, SI Analytics, Mainz, Germany). Data were captured and processed with a computer, using Titrisoft 3.2 software (SI Analytics, Mainz, Germany). For quality control, a certified reference material of known total alkalinity was used to calibrate the method (CRMs, Batch No. 160; supplied by the Marine Physical Laboratory, Scripps Institution of

Oceanography, USA), yielding TA values within  $5 \mu\text{mol kg}^{-1}$  of the certified value. Similar to photosynthesis, the maximum light calcification rates (max.  $G_{\text{Light}}$ ) and the initial slope of the Calcification-Irradiance curve ( $\alpha_G$ ) were determined. Here, the saturation irradiance ( $E_k$ ) was estimated as the ratio of max.  $G_{\text{Light}}/\alpha_G$ . In a posterior analysis, calcification was fitted against the respective gross photosynthesis for the different light levels and the initial slope of the curves was estimated using linear least-squares regression. Furthermore, mean ratios of max.  $G_{\text{Light}}/GP_{\text{max}}$  (mol  $\text{CaCO}_3$  precipitated per mol  $\text{O}_2$  evolved) were obtained by averaging the ratios of the light levels above saturation.

## pH-Drift Experiments and $\delta^{13}\text{C}$ Analysis

These experiments assessed the absence/presence of carbon-concentrating mechanisms (CCMs) in the studied rhodolith species. For this, rhodolith individuals ( $n=5$  per species and location) were incubated at their respective temperature and saturating light conditions ( $\sim 2-3E_k$ , derived from P-E curves) for 9-10.5 h and the pH of the seawater was measured with a pH meter (Metrohm, Switzerland), at the beginning and the end of the incubation. These experiments are based on the hypothesis that, if the seawater pH in the sealed incubation becomes greater than 9.0, no more  $\text{CO}_2$  is present, and it can be assumed that the species is able to uptake  $\text{HCO}_3^-$  during photosynthesis (Maberly, 1990). After the incubations, the chambers (without samples) were left open to the ambient air for re-calibration, making sure that the change in pH was due to the metabolism of the algae.

To identify potential differences among species regarding a preferential use of  $\text{CO}_2$  or bicarbonate (or both) for photosynthetic carbon assimilation (Maberly et al., 1992), the  $\delta^{13}\text{C}$  content of the algal tissue was analyzed. For this, rhodoliths ( $n=5$  per species and location) were dried (48 h at  $60^\circ\text{C}$ ) and afterwards placed in 1N HCl until the calcareous tissue was removed. The remaining tissue was rinsed with distilled water, dried again (48 h at  $60^\circ\text{C}$ ) and grounded into a fine powder, using a porcelain mortar and pestle. The samples were then weighed into pressed tin capsules and sent to the Stable Isotope Facility at University of California, Davis for analysis, using an Elementar vario MICRO cube elemental analyzer (Elementar Analysensysteme GmbH, Langensfeld, Germany) interfaced to a Sercon Europa 20-20 isotope ratio mass spectrometer (Sercon Ltd., Cheshire, UK).

## Inhibitor Studies

To gain insight into rhodolith carbon-concentrating and calcification mechanisms, and potential species-specific differences, their physiological responses to different inhibitors were measured. The specific inhibitor of PSII, 3-(3,4-Dichlorophenyl)-1,1-dimethylurea (DCMU, Sigma Aldrich) was dissolved in ethanol and added to the seawater to a final concentration of  $10 \mu\text{M}$ . Acetazolamide (AZ, Sigma Aldrich), a specific inhibitor of the external carbonic anhydrase, which mediates hydrolysis of  $\text{HCO}_3^-$ , was dissolved in 10 mM NaOH and used at a final concentration of 0.125 mM (Hofmann et al., 2016). The anion exchange inhibitor 4,4'-Diisothiocyano-2,2'-stilbenedisulfonic acid (DIDS, Sigma Aldrich) that blocks direct

$\text{HCO}_3^-$  uptake (Drechsler and Beer, 1991) was dissolved in dimethylsulfoxide (DMSO, Sigma Aldrich) and added at a final concentration of 0.6 mM. Ruthenium red (RR, Sigma Aldrich), a specific inhibitor of Ca-ATPase (Watson et al., 1971; Ip et al., 1991), and the Ca-channel inhibitor verapamil (VP, Sigma Aldrich) were both dissolved in DMSO and used at a final concentration of  $100 \mu\text{M}$  (de Beer and Larkum, 2001; Marshall and Clode, 2003). The final concentrations of DMSO and ethanol in the inhibitor treatments were 0.1%.

Rhodolith photosynthetic, respiratory and calcification rates were determined before and after inhibitor treatment by incubating individuals ( $n=5$  per species, location and inhibitor) at their respective temperatures for 0.5-1 h, at a saturating light intensity ( $\sim 2-3E_k$ , derived from P-E curves), and subsequently for 0.5 h in darkness, to determine maximum photosynthesis and respiration rates, respectively. Also, water samples were taken before and after each incubation for later estimation of calcification rates, as described above. Afterwards, with exceptions of the treatments with DCMU and AZ, the same samples were incubated with the inhibitors for 1 h in darkness, to ensure complete penetration into the cells, and then incubated again in light as described above. In the case of DCMU, before incubating the samples with the inhibitor, they were kept in darkness for 1-1.5 h to ensure complete oxidation of the electron-transport chain after the previous light incubation, as this inhibitor attaches to the  $Q_B$ -site within PSII. On the other hand, AZ was added directly after finishing the control measurements of the samples, without the inhibitor, and the incubations were repeated, as the effect of this inhibitor is immediate (membrane impermeable inhibitor).

## Statistical Analysis

Data were tested for normality and heteroscedasticity, using the Shapiro-Wilk and Levene's tests, respectively, and when required, log-transformed to normalize the data ( $R_D$ ,  $GP_{\text{max}}/R_D$ ,  $\alpha$ ,  $E_k$ ,  $E_c$ ,  $G_{\text{Light}}$ ,  $\alpha_G$ ). Physiological parameters were analyzed using one-way ANOVAs, with species as the between-subjects factor. In cases where significant differences were found, a Tukey's HSD *post hoc* test was conducted to determine significant groupings. Paired sample t-tests were used to compare the data from the inhibitor studies (before and after inhibitor treatment). To visualize differential inhibitor response profiles among rhodolith species, heat maps were generated using Python 3.10.2, along with the Pandas 1.3.5 (McKinney, 2011), Matplotlib 3.5.1 (Hunter, 2007) and Seaborn 0.11.2 (Waskom et al., 2020) libraries.

To visualize multivariate similarities in physiological characteristics across the range of species and locations under varying environmental contexts, RDA (Redundancy Analysis) ordinations, with the 'vegan' R package (Oksanen et al., 2020) and further customization *via* the 'ggord' R package ((Beck 2017), were carried out as a constrained ordination technique. Separate RDAs were implemented for both photosynthesis and calcification responses. Bi-plots were then constructed, displaying each rhodolith species, and for intra-specific comparison of *Phymatolithon* sp. from the different locations, including predictive variables (light, temperature) as vectors of

varying length and direction. The significance of these multivariate configurations was tested by the 'anova.cca' function, which also assessed the significance of each axis (component) to explain a significant amount of variation of the multivariate dataset. Variance inflation factors (VIFs) were always <5, indicating low collinearity among predictor variables for the RDA configuration in the bi-dimensional space.

## RESULTS

### Physiological Performance of Rhodoliths and Associated Environmental Drivers

Both photosynthesis and calcification increased when rhodolith species were exposed to increasing light intensities, until reaching a saturation point after which their rates stabilized around a maximum value (**Supplementary Figure S1**). However, the rate of these increases and the maximum values differed between the two processes and among the rhodolith species. When plotted against each other, this resulted in significant species-specific differences in the relationship between photosynthesis and calcification, specifically in the initial slopes of the photosynthesis-calcification curves at sub-saturating irradiances ( $<E_k$ ) and the maximum values reached ( $>E_k$ ) (**Figure 2; Table 2**). Calcification increased with photosynthesis at rates of 0.11 to 2.26 mol O<sub>2</sub> mol<sup>-1</sup> CaCO<sub>3</sub>, while maximum ratios of  $G_{\text{Light}}/GP_{\text{max}}$  ranged from 0.11 to 0.51 mol CaCO<sub>3</sub> mol<sup>-1</sup> O<sub>2</sub> (**Table 2**). Among species, the cold-temperature *Phymatolithon calcareum* expressed the slowest increase of calcification with photosynthesis and the lowest ratio of max.  $G_{\text{Light}}/GP_{\text{max}}$ , while the subtropical Brazilian species showed the fastest increases of CaCO<sub>3</sub> precipitation with photosynthesis and the highest  $G_{\text{Light}}/GP_{\text{max}}$  ratios (**Figure 2; Table 2**).

Differences among species were also reflected in their maximum photosynthetic performance ( $GP_{\text{max}}$ ), which was lowest in *Phymatolithon* sp. from habitats with low light availability (20-33 m), also associated with the lowest  $E_k$  and  $E_c$  values (**Figure 3A; Supplementary Table S1**). On the other hand, the highest  $GP_{\text{max}}$  values were found in species from contrasting latitudes, such as the cold-temperate *P. calcareum* and the subtropical *Phymatolithon* sp. from Arguineguín (14 m) and *Lithothamnion crispatum* from South Brazil (8 m). While there was no clear pattern in  $GP_{\text{max}}$  light calcification ( $G_{\text{Light}}$ ) was highest in the subtropical species, which inhabit depths under high light availability (20-21% of incident light), comprised of *Phymatolithon* sp. from Arguineguín (14 m) and the Brazilian species *Lithophyllum atlanticum*, *Melyvonnea erubescens*, and *L. crispatum* (**Figure 3B; Supplementary Table S2**). In contrast, dark calcification rates ( $G_{\text{Dark}}$ ) varied among species and seemed to be rather species-specific. For example, the three southern Brazilian species from the same location and depth showed large differences in  $G_{\text{Dark}}$ , varying between positive and negative values (indicating nighttime dissolution) (**Figure 3B**). The large variability was also reflected in the species'  $G_{\text{Dark}}/G_{\text{Light}}$  ratios, which ranged

between 0.09-0.33, with the highest ratios expressed by *Phymatolithon* sp. from Gran Canaria (**Supplementary Table S2**).

Multivariate analysis of the overall photosynthetic performance identified clear differences between the cold-temperate *P. calcareum* and the other species (except for *L. crispatum*), while the other two *Phymatolithon* species showed a high similarity (**Figure 4A**). The redundancy analysis revealed that light availability and temperature in the species' natural habitat collectively explained 36% of the total variance, with light exerting a larger influence, strongly correlating with  $E_k$ ,  $E_c$  and  $R_D$  (**Figure 4A; Supplementary Table S3**). Regarding calcification performance, the different *Phymatolithon* species showed similarities, but differed greatly from *M. erubescens* (**Figure 4B**). Here, light and temperature explained 18% of the variance, specifically exerting an influence on  $G_{\text{Light}}$  and  $\alpha_G$  (**Figure 4A; Supplementary Table S3**).

Intra-specific comparison of *Phymatolithon* sp. from four locations and depths showed no significant differences in the photosynthesis-calcification relationship, as rhodoliths from the different populations expressed similar initial slopes and max. ratios of  $G_{\text{Light}}/GP_{\text{max}}$ , also similar to the South Portuguese species *P. lusitanicum* (**Figure 2; Table 2**). On the other hand, an increasing trend in  $GP_{\text{max}}$ ,  $R_D$ ,  $G_{\text{Light}}$  and  $G_{\text{Dark}}$  was found with increasing light availability and temperature (**Figure 3; Supplementary Tables S1, S2**). Redundancy analysis showed that rhodoliths from Arguineguín (Gran Canaria) differed greatly in their general physiological performance, relative to those from other populations (**Figures 4C, D**). Here, site-specific light and temperature conditions explained 51% and 57% of the intra-specific variance in photosynthetic and calcification performance, respectively. In the case of photosynthesis, light and temperature exerted a similar influence on the photosynthetic variability among locations, correlating with  $NP_{\text{max}}$ ,  $GP_{\text{max}}$  and  $R_D$ . The variability in calcification parameters was mostly correlated to differences in temperature among the locations, with weaker influence of light availability (**Figures 4C, D; Supplementary Table S3**).

### Rhodolith CCM-Strategies

The  $\delta^{13}\text{C}$  values differed significantly among the rhodolith species (ANOVA,  $p < 0.0001$ ), ranging between -19.9‰ and -14.1‰ (**Figure 5A**). The highest values were found in the subtropical Brazilian species (-16.9 to -14.1‰), while the lowest values were expressed by *P. calcareum*, *P. lusitanicum* and *Phymatolithon* sp. (Bicudas, Porto Santo Island). These values were strongly and linearly related with the pH compensation points determined in six of the species ( $R^2 = 0.90$ ,  $p = 0.0027$ ), with all of them showing the capacity to reach  $\text{pH} \geq 9.0$  (**Supplementary Figure S2**), suggesting the presence of CCMs.

Inhibitor studies with DIDS and AZ, which inhibit active bicarbonate transport and  $\text{CA}_{\text{ext}}$ , respectively, indicated that the species expressed differences in their CCMs. While photosynthesis in the subtropical Brazilian species showed signs of active  $\text{HCO}_3^-$  transport (10-22% inhibition by DIDS), the other rhodolith species did not express any significant

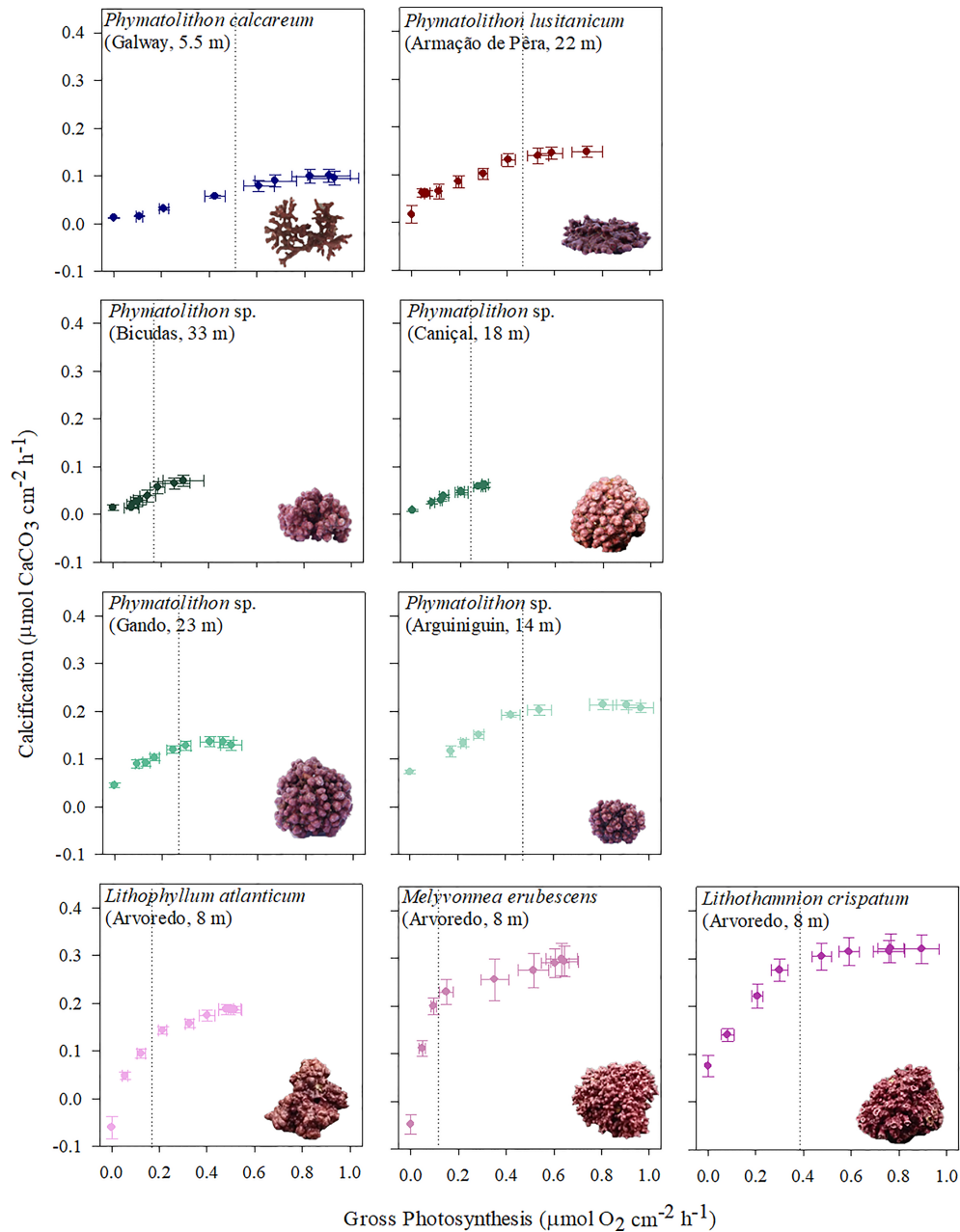


**FIGURE 2** | Photosynthesis-calcification relationships for Atlantic rhodolith species (location, depth), obtained from light curves (dotted line indicates  $E_k$ ). Data points represent mean  $\pm$  SE ( $n=5$ ).

changes in photosynthetic activity under this inhibitor treatment (Figure 5B; Supplementary Table S4). In contrast, the AZ-treatment indicated that photosynthesis in all species relied on the activity of the  $CA_{ext}$ , as its inhibition significantly decreased  $GP_{max}$  (Figure 5B). The data showed that photosynthesis was generally 50-60% lower in absence of  $CA_{ext}$  activity, though *Phymatolithon* sp. from Caniçal (Madeira Island) showed a lesser effect (33% lower  $GP_{max}$ ) (Figure 5B; Supplementary Table S4).

## Rhodolith Calcification Mechanisms

The use of different inhibitors revealed a highly dynamic pattern regarding the importance of specific processes for rhodolith calcification. All species showed a strong correlation of light calcification and photosynthesis, as the former experienced a significant decrease (68-91% lower  $G_{Light}$ ) upon inhibition of the latter, which was also directly related to the species' decline in calcification in darkness ( $G_{Dark}$ ; Figure 6). In fact, in most

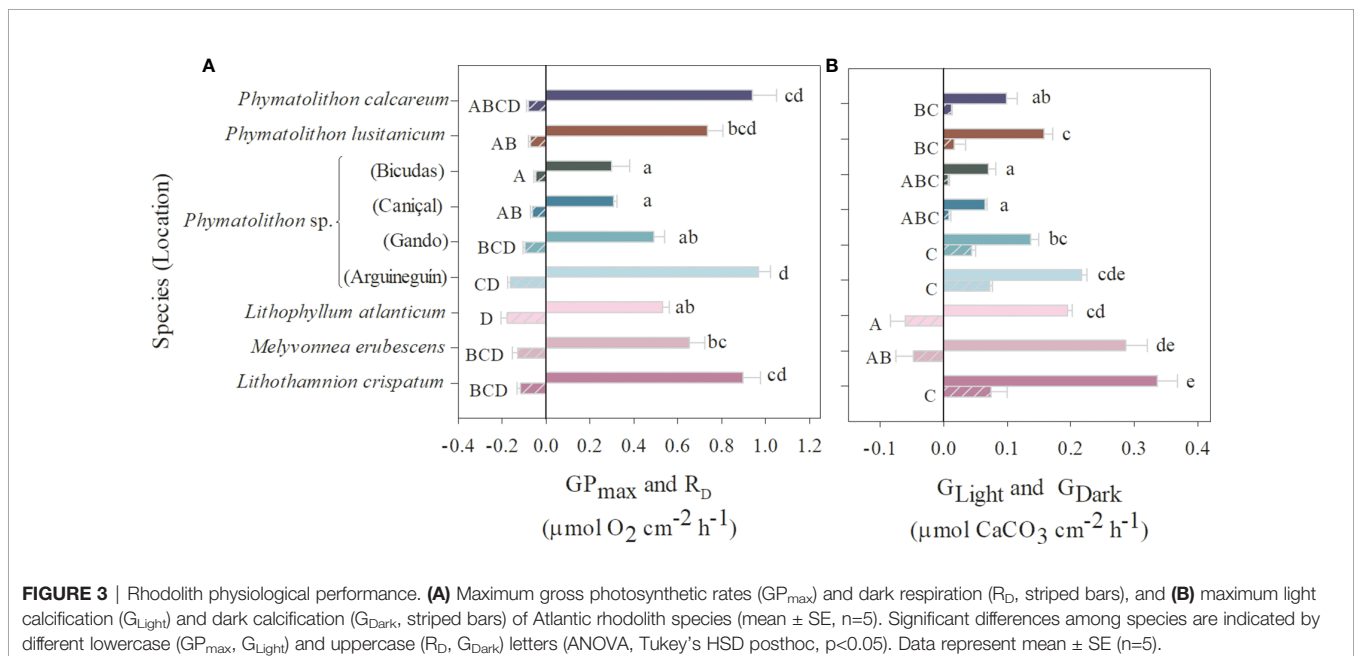
**TABLE 2** | Comparison of parameters derived from photosynthesis-calcification relationships in different Atlantic rhodolith species (**Figure 2**).

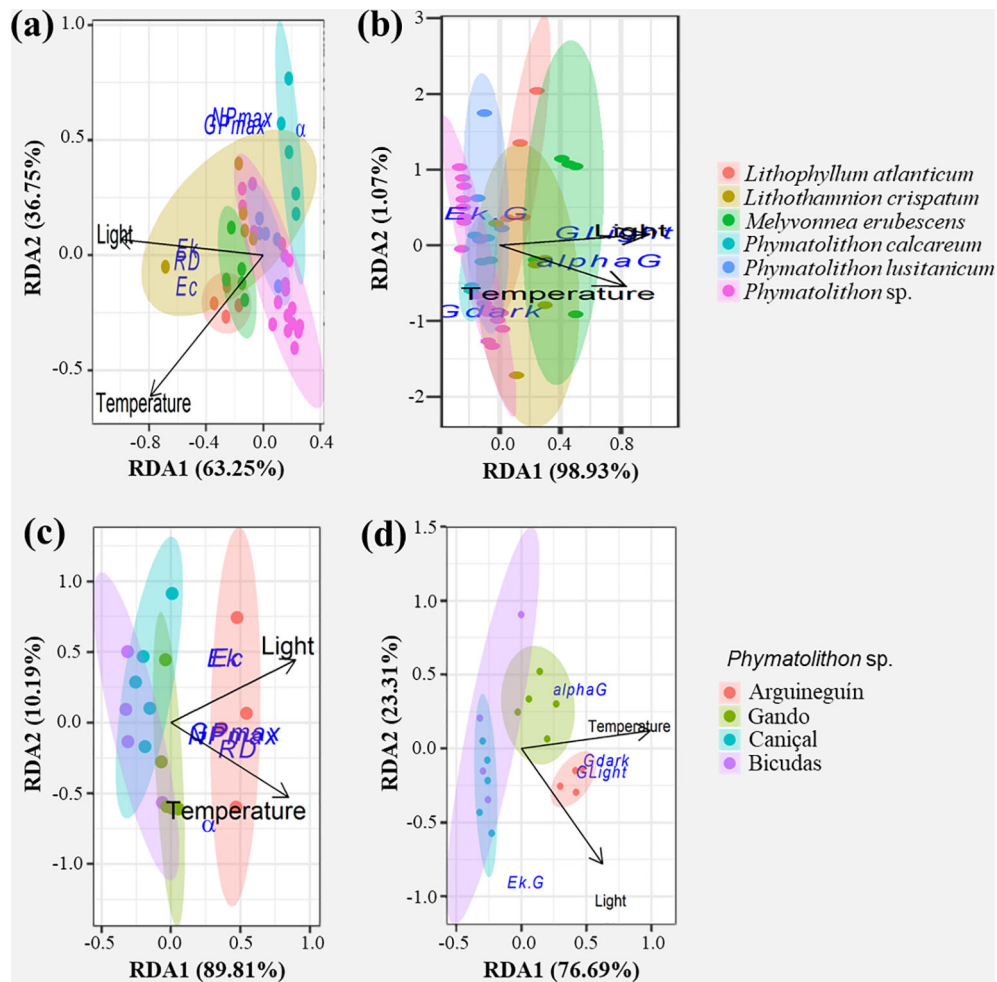
Species	Slope of increase of $G_{\text{Light}}$ with GP	$G_{\text{Light}}/GP_{\text{max}}$
<b>Cold-temperate</b>		
<i>Phymatolithon calcareum</i>	$0.114 \pm 0.007^a$	$0.11 \pm 0.01^a$
<b>Warm-temperate</b>		
<i>Phymatolithon lusitanicum</i>	$0.248 \pm 0.015^b$	$0.24 \pm 0.02^{bc}$
<i>Phymatolithon</i> sp. (Bicudas)	$0.225 \pm 0.053^{ab}$	$0.34 \pm 0.07^{bcd}$
<i>Phymatolithon</i> sp. (Canical)	$0.193 \pm 0.019^{ab}$	$0.21 \pm 0.02^b$
<b>Subtropical</b>		
<i>Phymatolithon</i> sp. (Gando)	$0.313 \pm 0.044^{bc}$	$0.33 \pm 0.03^{cde}$
<i>Phymatolithon</i> sp. (Arguineguín)	$0.259 \pm 0.033^b$	$0.24 \pm 0.02^{bc}$
<i>Lithophyllum atlanticum</i>	$1.261 \pm 0.143^d$	$0.39 \pm 0.02^{de}$
<i>Melyvonnea erubescens</i>	$2.262 \pm 0.156^d$	$0.51 \pm 0.08^e$
<i>Lithothamnion crispatum</i>	$0.705 \pm 0.226^c$	$0.38 \pm 0.02^{de}$
ANOVA	$F=42.57, p<0.0001$	$F=24.34, p<0.0001$

Table Legend: Initial linear slope of the increase of calcification with photosynthesis at irradiances  $<E_k$  ( $\text{mol O}_2$  precipitated  $\text{mol}^{-1} \text{CaCO}_3$ ) and mean ratio of maximum light calcification ( $G_{\text{Light}}$ ) to gross photosynthesis ( $GP_{\text{max}}$ ) at saturating irradiances ( $>E_k$ ) ( $\text{mol CaCO}_3$  precipitated  $\text{mol}^{-1} \text{O}_2$ ). Data represent mean  $\pm$  SE and significant differences among species (ANOVA, Tukey's HSD posthoc,  $p<0.05$ ) are indicated by different letters.

species responded with a decline of  $G_{\text{Light}}$  under photosynthesis inhibition and in darkness, except for *M. erubescens* and *L. atlanticum* that expressed negative dark calcification rates. Similarly to photosynthesis, all species showed a significant decrease in  $G_{\text{Light}}$  under  $CA_{\text{ext}}$  inhibition (by 51-125%, **Figure 7; Supplementary Table S4, S5**). To distinguish between direct effects of  $CA_{\text{ext}}$  inhibition on calcification and indirect effects due to a decline in photosynthesis, changes in  $GP_{\text{max}}/G_{\text{Light}}$  ratios were analyzed, where non-significant changes in the ratios indicated only indirect effects on calcification due to photosynthesis decline. The results indicated that for the Brazilian species the recorded decline in calcification upon  $CA_{\text{ext}}$  inhibition was the sole result of an indirect effect due to the decline in  $GP_{\text{max}}$ . On the other hand, the other rhodolith species exhibited a larger decrease in  $G_{\text{Light}}$ , compared to  $GP_{\text{max}}$ , which suggested a direct role of  $CA_{\text{ext}}$  for calcification (**Figure 7; Supplementary Tables S4-S6**).

Likewise, the inhibition of active bicarbonate transport caused different responses among the species. While the absence of  $\text{HCO}_3^-$  transport did not cause significant effects in calcification in *Phymatolithon* sp. from Arguineguín (Gran Canaria), it induced a significant decrease in  $G_{\text{Light}}$  in the same species from Canical (Madeira Island), in *P. lusitanicum*, and in the three Brazilian species, though the magnitude of the effect varied greatly (from 15 to 73% decrease). Comparing these findings to the inhibitor effect on species' photosynthesis, it suggests the involvement of active bicarbonate transport in calcification, but not in photosynthesis, in the species from Europe and the coast of northwestern Africa (**Figure 7; Supplementary Tables S4, S5**). In the case of the Brazilian species, where significant responses in both photosynthesis and calcification under inhibitor treatment were found, the comparison of  $GP_{\text{max}}/G_{\text{Light}}$  ratios indicated that active  $\text{HCO}_3^-$  transport was directly involved in both processes in *L. atlanticum* and *L. crispatum*, but



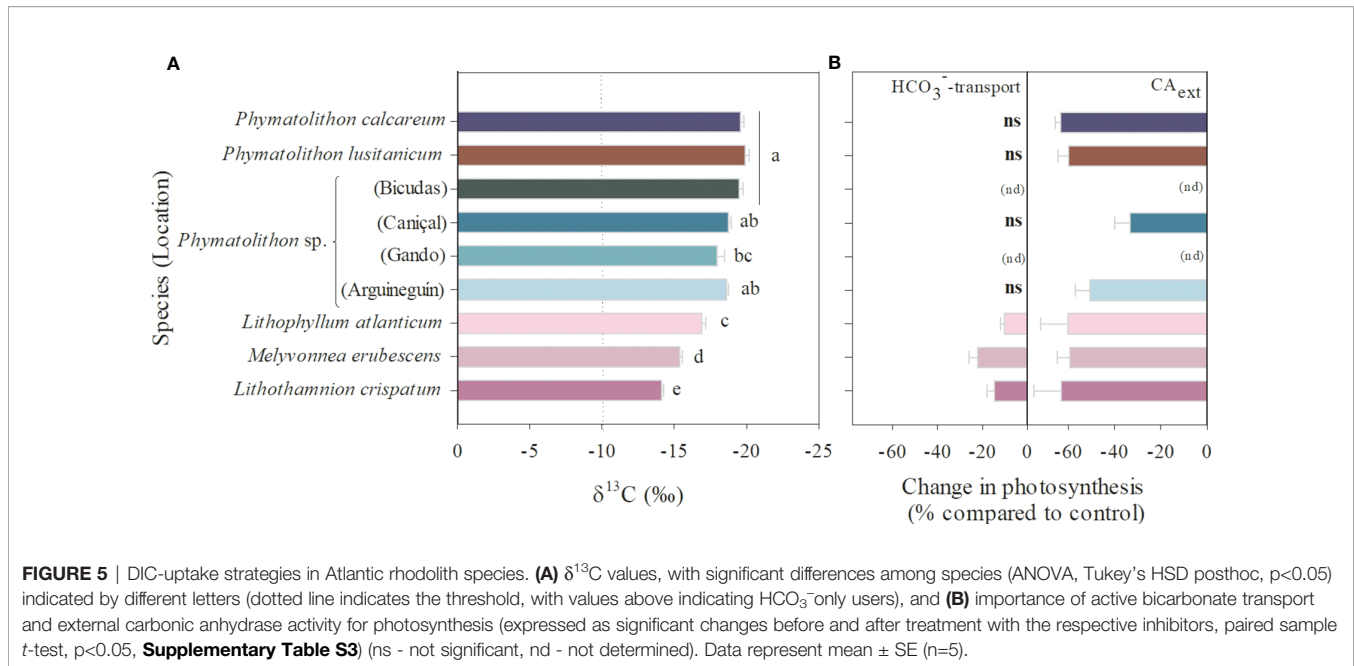


**FIGURE 4** | Influence of environmental factors on rhodolith physiological performance. Redundancy analysis (RDA) biplots show the contribution of local environmental conditions (light availability, temperature) to the variation in photosynthetic (A, C) and calcification parameters (B, D) of all studied Atlantic rhodolith species (A, B) and of *Phymatolithon* sp. sampled in different locations (C, D). Arrows represent correlations between environmental variables and the RDA axes, with arrow length indicating the strength of the correlation. Response variables are indicated by circles ( $GP_{max}$ ,  $NP_{max}$  - max. gross and net photosynthesis;  $R_D$  - dark respiration;  $\alpha$ ,  $\alpha_{G-}$  photosynthetic and calcification efficiency under subsaturating light intensities;  $E_k$ ,  $E_c$  - saturating and compensatory light intensity;  $G_{Light}$ ,  $G_{dark}$  - max. light and dark calcification).

not in *M. erubescens*, in which the inhibitor effect on calcification seemed to be caused exclusively by the decline in photosynthesis (Supplementary Table S6). Surprisingly, *P. calcareum* showed an opposite response to DIDS, with a 97% increase in calcification (Figure 7B; Supplementary Table S5). The cold-temperate *P. calcareum* also differed from the others regarding the importance of Ca-channel and -ATPase for calcification, as it did not exhibit any significant effects upon their inhibition (Figure 7). Among the other species, the importance of these two transporters varied greatly. Some species exhibited a significant decline in calcification under Ca-channel and/or Ca-ATPase inhibition, while others did not. For example, little to no significant effect of Ca-channel inhibition was found in two of the subtropical Brazilian species (*L. crispatum* and

*L. atlanticum*, respectively), while the inhibition of the Ca-ATPase did not result in significant effects in *Phymatolithon* sp. from Arguineguín (Gran Canaria) and *M. erubescens* from Brazil (Figure 7).

When comparing the effects of the different inhibitors, at an intra-specific level in *Phymatolithon* sp. from two locations, the results show that the calcification responses varied greatly, especially regarding the importance of DIDS-sensitive bicarbonate transport and Ca-ATPase (Figure 7; Supplementary Table S5). Also,  $CA_{ext}$  was seemingly more important for calcification in the rhodoliths from Arguineguín (Gran Canaria), compared to those from Caniçal (Madeira Island) (Figure 7B; Supplementary Table S5), also shown by its larger changes in  $GP_{max}/G_{Light}$  ratios (Supplementary Table S6).



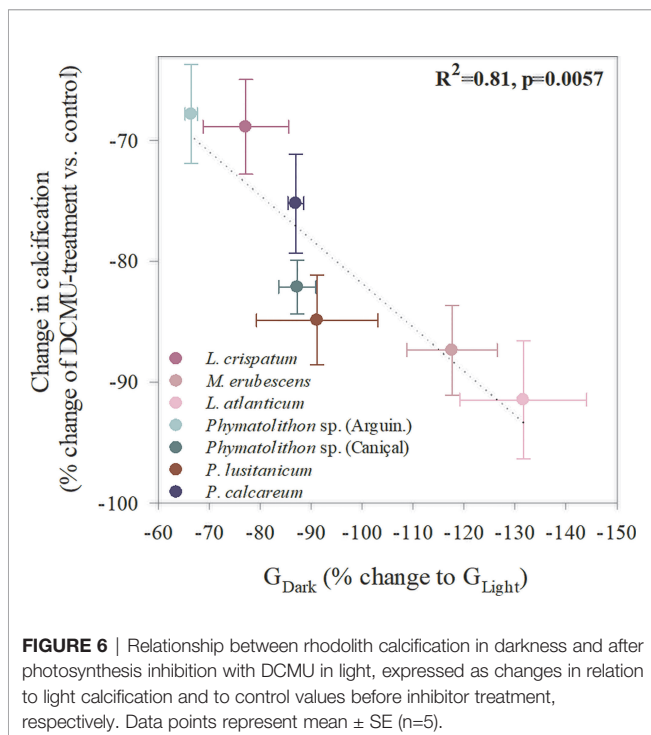
## DISCUSSION

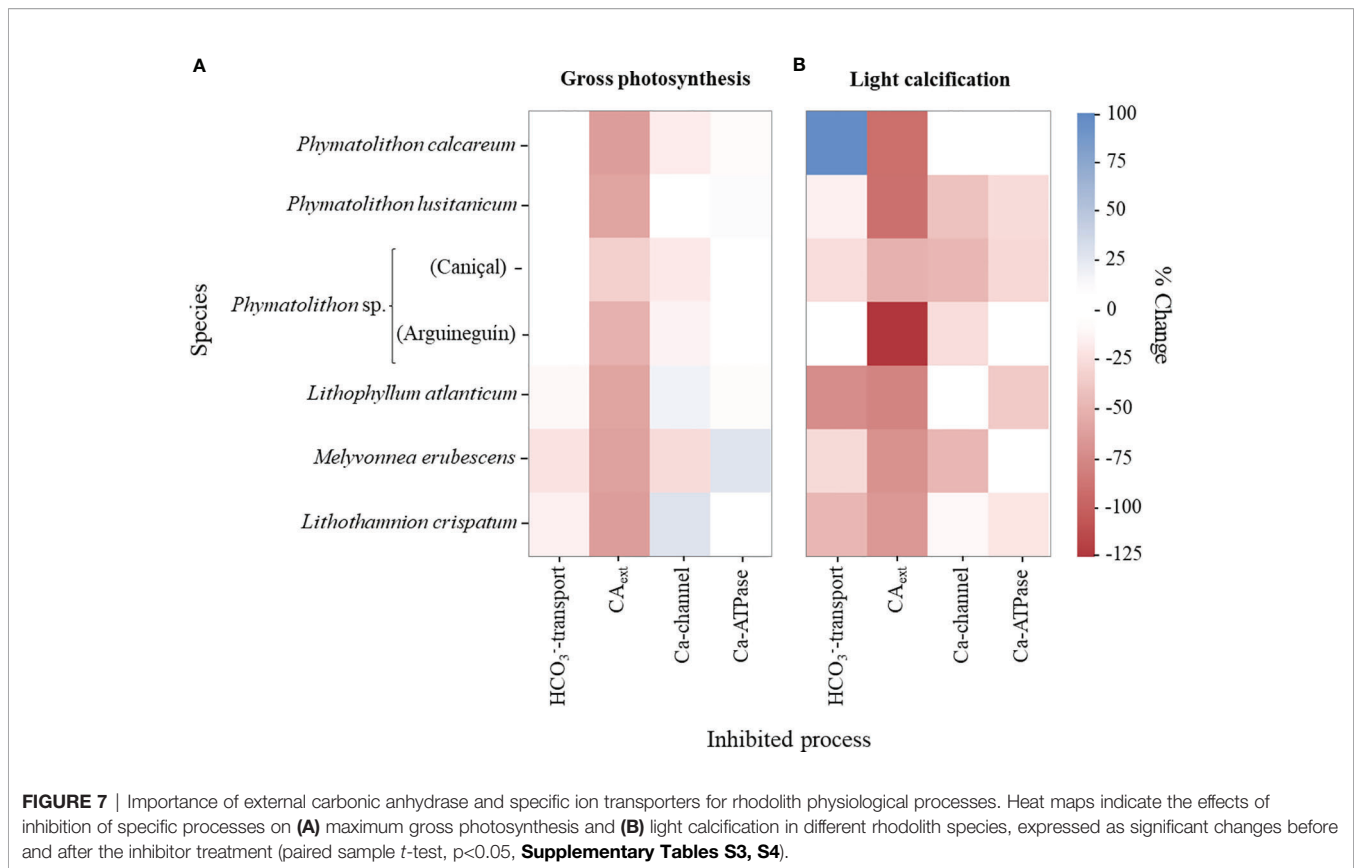
This study demonstrated that rhodoliths express high inter-specific variability in their physiological performance and underlying mechanisms. Specifically, the different species show a high plasticity in the strength of the coupling of photosynthesis and calcification, in the CCM-strategies and in the ion transporters and enzymes involved in calcification. Furthermore, intra-specific comparisons suggest that this

variability is at least partially modulated by local environmental conditions.

## Rhodolith Physiological Performance and the Importance of Environmental Conditions

Overall, our findings regarding the importance of temperature and light for rhodolith performance agrees with recently published distributional models, identifying these factors as two of the main drivers of rhodolith distribution (Carvalho et al., 2020; Simon-Nutbrown et al., 2020; Fragkopoulou et al., 2021; Sissini et al., 2021). At the inter-specific level, rhodolith photosynthetic performance was mainly driven by light, but very little by temperature and hence, it did not show a latitudinal pattern. On the other hand, temperature and light were identified as strong environmental drivers for rhodolith light calcification, which was reflected in increased  $G_{\text{Light}}$  towards lower latitudes. This is consistent with higher summer calcification rates reported for cold- and warm-temperate rhodolith species (Sordo et al., 2020; Qui-Minet et al., 2021). Dark calcification rates, on the other hand, seemed to be related to species identity rather than environmental conditions, which is in accordance with other comparative studies for crustose coralline algae (Chisholm, 2000) and rhodoliths (Qui-Minet et al., 2021; Schubert et al., 2021a). In their comparative study of three rhodolith species, Qui-Minet et al. (2021) also showed that  $G_{\text{Dark}}$  can vary seasonally, from negative rates in winter to positive rates in summer, though the relative differences between species were maintained. This agrees with our findings of increased  $G_{\text{Dark}}$  with temperature at the intra-specific level in *Phymatolithon* sp. (**Figure 3B**). In fact, temperature was the main driver for the calcification differences in this species from different locations. The variability in the photosynthetic performance was induced by temperature and light availability,





resulting in higher physiological rates of the specimens collected at the shallowest subtropical rhodolith bed (Arguineguin).

Species identity has a strong influence on the relationship between photosynthesis and calcification, as evidenced by significant differences among species and, specifically, those found among species from the same location (see *L. atlanticum*, *M. erubescens*, *L. crispatum*). This agrees with a recent comparison among the temperate rhodolith species, *Lithothamnion corallioides*, *Lithophyllum incrustans* and *Phymatolithon calcareum*, from the same habitat, which also exhibited significant differences in their  $G_{\text{Light}}/GP_{\text{max}}$  ratios (Qui-Minet et al., 2021). This species-specific dependence of calcification on photosynthesis was also supported by differences in the decline of the former in the absence of the latter, either by using inhibitors, or under dark conditions (discussed in more detail below). Additionally, comparison at the intra-specific level suggests that local environmental conditions induced some variability in the photosynthesis-calcification relationship, as evidenced by differences found among *Phymatolithon sp.* from different locations. The likely cause for the variability was the differential influence of environmental factors on the two processes, as differences in calcification among locations were mostly driven by temperature, while variability in photosynthetic performance was induced, to a similar extent, by both light and temperature. Similar findings have also been reported for the temperate rhodolith *Lithothamnion corallioides*, which not only showed variable  $G_{\text{Light}}/GP_{\text{max}}$  ratios among different locations,

but also between seasons (0.40–0.53 in winter, 0.26–0.32 in summer) (Qui-Minet et al., 2021).

## Rhodolith CCM Strategies

Marine macroalgae can express three mechanisms of DIC assimilation: (1) diffusive CO<sub>2</sub> uptake, (2) CO<sub>2</sub> uptake dependent on CA<sub>ext</sub> catalyzed dehydration of HCO<sub>3</sub><sup>-</sup>, and (3) direct transport of HCO<sub>3</sub><sup>-</sup> (Johnston, 1991). The degree to which these mechanisms are used by an alga determines the extent to which the alga can use bicarbonate as inorganic carbon source, to maintain maximum, or near maximum, photosynthetic performance during times when DIC becomes limited due to high photosynthesis and/or the presence of a thick DBL.

Our findings, as well as previous studies, demonstrate that rhodoliths express active CCMs, but also a variability in  $\delta^{13}\text{C}$  values associated to the species and/or environmental conditions (Hofmann and Heesch, 2018; Hofmann et al., 2018). All the rhodolith species studied here expressed  $\delta^{13}\text{C}$  values that identified them as both CO<sub>2</sub> and bicarbonate users ( $\delta^{13}\text{C} = -30$  to  $-10\%$ , Maberly et al., 1992). Together with the pH-drift experiments, this demonstrated that the species were able to raise the pH > 9.0, at which DIC in form of CO<sub>2</sub> is functionally 0, suggesting the presence of CCMs. This agrees with reports of  $\delta^{13}\text{C}$  in other rhodoliths and crustose coralline algae (e.g., Wang and Yeh, 2003; Cornwall et al., 2015; Diaz-Pulido et al., 2016; Hofmann and Heesch, 2018; Zweng et al., 2018; Bergstrom et al., 2020).

The non-diffusive and diffusive DIC uptake in algae vary and can involve both the active transport of  $\text{HCO}_3^-$  and the catalytic conversion of  $\text{HCO}_3^-$  to  $\text{CO}_2$  by CA, with subsequent passive diffusion of  $\text{CO}_2$ , respectively. Here, the use of specific inhibitors demonstrated that all studied rhodolith species relied on the activity of  $\text{CA}_{\text{ext}}$  for photosynthesis, though its importance varied among species. In addition, the subtropical Brazilian species expressed active  $\text{HCO}_3^-$  transport as CCM, as demonstrated by the significant decline in photosynthesis under DIDS-treatment. This evidently increased the carbon-concentrating efficiency in these species, as shown by their higher pH compensation point (see **Supplementary Figure S2**). Overall, it agrees with the seemingly prevalent importance of  $\text{CA}_{\text{ext}}$  for inorganic carbon assimilation in coralline algae (Hofmann et al., 2016; Hofmann et al., 2018; Hofmann and Heesch, 2018; Zweng et al., 2018). On the other hand, the presence/absence of a DIDS-sensitive active  $\text{HCO}_3^-$  transport appears to be more variable among species (this study; Hofmann et al., 2016; Hofmann et al., 2018; Zweng et al., 2018), though the here demonstrated importance of both  $\text{CA}_{\text{ext}}$  and active DIDS-sensitive bicarbonate transport in the subtropical Brazilian species agree with those in other tropical coralline algae (Hofmann et al., 2016; McNicholl et al., 2019). These findings were consistent with the higher (less negative)  $\delta^{13}\text{C}$  values of the subtropical Brazilian species, while the lower (more negative) values of the other species may indicate a higher reliance on  $\text{CA}_{\text{ext}}$  activity (Mercado et al., 2009). Nevertheless, the  $\delta^{13}\text{C}$  values identified all species as both bicarbonate and  $\text{CO}_2$  users, suggesting the presence of other bicarbonate uptake mechanisms, insensitive to DIDS.

CCM strategies in algae, and the degree to which they are expressed, are modulated by a variety of environmental conditions (e.g., light, temperature, pH, salinity, nutrients; Beardall et al., 1998; Beardall and Giordano, 2002; Giordano et al., 2005). As for the influence of pH conditions, these can also be modified by the organisms themselves, as photosynthetic activity increases seawater pH and simultaneously decreases  $\text{CO}_2$  concentration and it has been shown previously that this combination increased markedly the expression of  $\text{CA}_{\text{ext}}$  activity (Berman-Frank et al., 1995; Berman-Frank et al., 1998). Thus, when considering the demonstrated effect of algal morphology on DBL thickness and related pH dynamics (Hurd et al., 2011; Cornwall et al., 2013; Cornwall et al., 2014; Schubert et al., 2021a), morphology may be one of the factors driving species' differences in CCM strategies.

A recent study on the Brazilian rhodolith species showed the effect of their morphology on DBL thickness and associated thallus surface pH dynamics (Schubert et al., 2021a). The species studied here differ in their general morphology (round, thin-branched, flattened), but also in the rugosity of the thallus surface, as indicated by their surface area to dry weight ratios. Brazilian rhodoliths have higher ratios, related to a higher number and length of protuberances, than the other studied species with similar round morphologies (not considering *P. calcareum* and *P. lusitanicum*, which have thin-branched and flattened morphologies, respectively) (**Supplementary Table S7**). These differences might explain the greater diversity

and importance of CCMs, such as the presence of a DIDS-sensitive direct entry of  $\text{HCO}_3^-$  in the Brazilian species, which was absent in the others. The morphology-induced built-up of thicker DBLs results in an increase in the lengths of  $\text{CO}_2$  diffusive pathway, which together with a high photosynthetic activity will lead to carbon limitation. Thus, the lower morphological complexity of species from Europe and the coast of northwestern Africa with similar round morphologies, suggests thinner DBLs and consequently shorter  $\text{CO}_2$  diffusion pathways. This agrees with the importance of  $\text{CA}_{\text{ext}}$  and a higher reliance on diffusive  $\text{CO}_2$  uptake. In contrast, in the three Brazilian species (with thicker DBLs) CCMs are required to maintain photosynthetic activity. Indeed, the increase in the  $\text{pH}_{\text{DBL}}$  between the rhodolith protuberances under light conditions found previously in the Brazilian species (mean=0.33-0.55 units higher than bulk seawater pH; Schubert et al., 2021a) might explain the found expression of an active  $\text{HCO}_3^-$  transport, as it is a carbon uptake mechanism that can be induced by high external pH values (Axelsson et al., 1995). Hence, the higher  $\delta^{13}\text{C}$  of the Brazilian species could be explained by their higher morphological complexity that drives the formation of thicker DBLs and results in an increase in the length of  $\text{CO}_2$  diffusion pathways and the need for CCMs ( $\text{CA}_{\text{ext}}$  and active  $\text{HCO}_3^-$  uptake). Based on this premise, and the assumption that coralline algae with lower CCM capacity have a higher diffusive  $\text{CO}_2$  uptake (Bergstrom et al., 2020), it could be hypothesized that among the studied species, morphologically less complex species, such as *Phymatolithon* sp. from Caniçal (Madeira Island), rely to a higher degree on diffusive  $\text{CO}_2$  entry as DIC uptake strategy, as evidenced by its lower pH compensation point and lesser importance of  $\text{CA}_{\text{ext}}$  for photosynthesis. This may also be the case in *P. lusitanicum*, which expresses a flattened morphology that is not conducive to thick DBLs and hence, diffusive  $\text{CO}_2$  uptake may also be more important in this species, as supported by its lower  $\delta^{13}\text{C}$  values.

## Rhodolith Calcification Mechanism

Overall, inhibitor studies in different groups of calcifiers have shown that  $\text{CA}_{\text{ext}}$ , bicarbonate transporters, Ca-channels and Ca-ATPase are involved in carbonate precipitation (e.g., Dubois and Chen, 1989; McConnaughey, 1989; McConnaughey and Falk, 1991; Allemann and Grillo, 1992; Tambutté et al., 1996; Comeau et al., 2013; Hofmann et al., 2016; Hofmann et al., 2018). The present study supports this, though it also clearly shows that rhodoliths express inter-specific differences, not only in the dependence of calcification on photosynthesis, but also the importance of  $\text{CA}_{\text{ext}}$  and specific ion-transporters for calcification.

Firstly, our results showed a high variability in the decline of calcification upon photosynthesis inhibition, suggesting species-specific differences in the strength of the link between these two processes. Additionally, environmental conditions seem to exert an influence on this relationship, as shown in *Phymatolithon* sp., with rhodoliths from Arguineguín (Gran Canaria) showing a lower dependence of calcification on photosynthesis, compared to the same species from Caniçal (Madeira Island). The similar decrease in calcification rates in darkness (when compared to

$G_{\text{Light}}$ ), and upon photosynthesis inhibition in light in most of the studied species, points towards not only a photosynthesis- but also light-independent mechanism that enables rhodoliths to maintain positive calcification rates in the absence of photosynthesis in light, as well as in darkness. In this context, evidence for a  $\text{HCO}_3^-/\text{H}^+$  symport that moves protons away from the calcification site under both light and dark conditions, resulting in an increase in surface pH, has been found in the Arctic rhodolith *Lithothamnion glaciale* (Hofmann et al., 2018). The exceptions among the studied species were the two Brazilian species *L. atlanticum* and *M. erubescens*, in which this potential light-independent mechanism was either less effective (operating at a slower rate) or absent, resulting in carbonate dissolution in darkness and an almost complete cease of light calcification upon photosynthesis inhibition. As a recent comparative microsensor study showed, this feature is related to a pH decline at the thallus surface in darkness in these two species that was not found in *L. crispatum* from the same location (Schubert et al., 2021a). The magnitude of night-time decalcification was shown to be directly related to the pH decline in darkness, which was larger in *L. atlanticum*, resulting in higher carbonate dissolution, compared to *M. erubescens*. In previous studies, Hofmann et al. (2016; Hofmann et al., 2018) provided evidence that some coralline algae present a light-mediated, but photosynthesis-independent proton pump. The presence of such a mechanism might decrease the dependence of calcification on photosynthesis and could explain the significantly faster increase of calcification upon light exposure ( $\alpha_G$ ) in the two aforementioned species, compared to the other species.

Secondly, differences among species were also found regarding the importance of bicarbonate-transporters and  $\text{CA}_{\text{ext}}$  for calcification. Our results show that they not only supported photosynthesis, but also calcification in some rhodolith species, while in others they were important only for one of those processes (Figure 8). Noteworthy here was the finding of the direct involvement of  $\text{CA}_{\text{ext}}$  in photosynthesis and calcification in the temperate and subtropical *Phymatolithon* species, while in the subtropical Brazilian species the activity was seemingly important only for photosynthesis and hence,

only indirectly for calcification. Generally, it is assumed that  $\text{CA}_{\text{ext}}$  is involved directly in coralline algal calcification, by elevating the pH due to removal of  $\text{H}^+$  through  $\text{HCO}_3^-$  dehydration ( $\text{HCO}_3^- + \text{H}^+ \leftrightarrow \text{CO}_2 + \text{H}_2\text{O}$ ), with the resulting  $\text{CO}_2$  diffusing into the cells to be used for photosynthesis (Borowitzka, 1987; Koch et al., 2013; Hofmann et al., 2018; McNicholl et al., 2019). Though, in the proposed models, no clear distinction is made between its direct and indirect importance (activity related to photosynthetic DIC uptake) and more studies are needed to differentiate the functional role of  $\text{CA}_{\text{ext}}$  in coralline algal calcification. Another surprising difference found among the studied species was related to the importance of DIDS-sensitive active  $\text{HCO}_3^-$  transport. Even though this transporter did not play a role for photosynthesis in the species from Europe and those off the coast of northwestern Africa, in some of them it seemed to play a role in calcification (Figure 8). Yet, the extent to which this transporter was involved in calcification differed greatly among species. Furthermore, in the cold-temperate *P. calcareum* and the subtropical *Phymatolithon* sp. (Arguineguín), the DIDS-sensitive bicarbonate transporter did not play a role in neither photosynthesis nor calcification. In the case of the latter species, this also suggests an intra-specific variability in the degree to which calcification depends on this bicarbonate transporter. *Phymatolithon* sp. from Arguineguín (Gran Canaria) did not express active DIDS-sensitive bicarbonate transport, but its calcification depended highly on the activity of  $\text{CA}_{\text{ext}}$ , while in the same species from Caniçal (Madeira Island) both mechanisms were important to a certain degree (Figure 8).

Thirdly, a large variability among rhodolith species regarding calcium transporters was found. Generally, it is assumed that Ca-influx to cells occurs through voltage sensitive Ca-channels, while Ca-efflux is associated to a Ca-ATPase (McConnaughey, 1989). The latter has been shown to be associated with calcification in corals and algae (e.g., Okazaki, 1977; Okazaki et al., 1984; Kingsley and Watabe, 1985). The “trans” calcification mechanism model proposed for these calcifiers suggests that Ca-ATPase supplies  $\text{Ca}^{2+}$  to and removes  $\text{H}^+$  from the site of calcification, resulting in an increase in pH and  $[\text{Ca}^{2+}]$  that

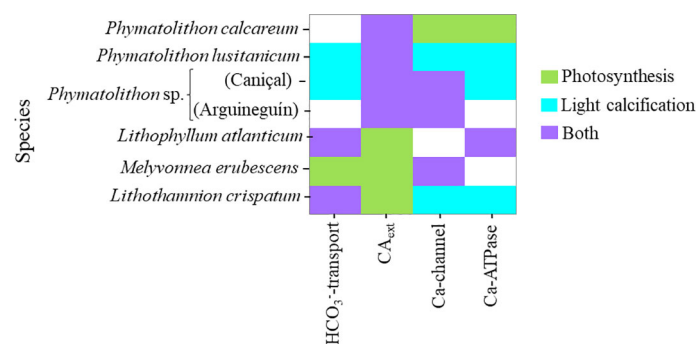


**FIGURE 8** | Summarized overview of the importance of  $\text{CA}_{\text{ext}}$  and specific ion-transporters for rhodolith photosynthesis and/or calcification, based on inhibitor effects and accounting for declines in calcification caused indirectly by inhibitor effects on photosynthesis (“Both”- inhibitor effect on both processes, but larger in calcification, indicating direct effect on the latter; **Supplementary Tables S3–S5**).

favors  $\text{CaCO}_3$  precipitation (McConnaughey and Falk, 1991; McConnaughey and Whelan, 1997). Among the different groups of calcareous algae, Ca-ATPase has been shown to be specifically relevant in coralline algae (Okazaki, 1977). Evidence for its involvement in calcification has been provided by a recent microsensor study in a crustose coralline alga (Hofmann et al., 2016). Here,  $\text{Ca}^{2+}$  and pH dynamics recorded at the algal thallus surface under different light conditions, clearly demonstrated the presence of an active Ca-efflux and  $\text{H}^+$ -influx into the cells in light, resulting in an increase of surface pH, and the inverse pattern in darkness. It also agrees with our findings of a significant decline in calcification upon ATPase-inhibition. Still, this effect was found only in four of the rhodolith species (Figure 8), indicating that its expression might not be universal in all species of this group and/or driven by the environment (see *Phymatolithon* sp. from Caniçal and Arguineguin). For example, the lack of any effects of Ca-ATPase inhibition in *M. erubescens* suggests that this species may express a different  $\text{Ca}^{2+}/\text{H}^+$  exchanger to regulate pH at the calcification site.

The rhodolith species also exhibited differences regarding the importance of Ca-channels, as found through the treatment with verapamil. This inhibitor is specific for L-type (voltage-dependent, with long-lasting activation) Ca-channels (Triggle, 2006) and the lack of effects in *L. atlanticum* in either photosynthesis, or calcification, may suggest a different type of Ca-channel in this species, insensitive to verapamil. Differences in Ca-channels have been reported also for other calcareous macrophytes, such as *Chara* sp. and *Halimeda discoidea* Decaisne. The calcium flux in *Chara* spp. has been found to be insensitive to verapamil, but showed sensitivity to nifedipine, an inhibitor of N-type Ca-channels (Reid and Smith, 1992; Stento et al., 2000). On the other hand, neither the inhibition of L- nor N-type Ca-channels had an effect on  $\text{Ca}^{2+}$  dynamics in *H. discoidea* (de Beer and Larkum, 2001). Altogether, our results show a highly diverse and dynamic pattern regarding the expression of calcium transporters (Ca-channel, Ca-ATPase), which seems to be related to the species, but based on the intra-specific comparison of *Phymatolithon* sp., can also be modulated by the environment (Figure 8). It agrees with the reported high variability in the presence/absence of gene sequences associated to calcium transporters, such as Ca-ATPase and  $\text{Ca}^{2+}/\text{H}^+$  exchangers in Rhodophyta (Schönknecht, 2013; Tong et al., 2021).

## CONCLUSIONS

Our study shows that rhodolith species, and most likely coralline algae in general, display a large variability in (a) their general physiology and associated mechanisms, and (b) their maximum physiological performance. The former has implications for potential differences in the response to climate-change associated factors, such as ocean acidification. Large variability in the photosynthesis-calcification relationships and calcification mechanism suggests species' differences in their capacity to maintain a high pH-environment at the calcification site and,

consequently, in their susceptibility to OA. Our findings did not identify a general pattern for all species, but rather a species-specific interplay of mechanisms, driven by species physiological and morphological traits, but also by intra-specific modulation of acclimation/adaptation to environmental conditions. Furthermore, the large variability in maximum physiological performance among rhodolith species, which is modulated by light and/or temperature, suggests differences in net productivity not only at the individual, but also scaled up rhodolith-bed community level at different latitudes.

## DATA AVAILABILITY STATEMENT

The original contributions presented in the study are included in the article/Supplementary Material. Further inquiries can be directed to the corresponding author.

## AUTHOR CONTRIBUTIONS

NS and JS developed the concept, including the method and approach to be used; NS, VS, PH, PN, CR, FO-F, FT, FE, KS, and JS conducted the sampling collections; NS, VS, and JS conducted the experiments, NS performed sample analysis, NS, FT, and VS performed the data analysis; VP and LG performed the molecular identification of the rhodolith species, NS wrote the original draft of the article, supported by all authors who contributed to the writing, reviewing, and editing of the paper. All authors have read and agreed to the published version of the manuscript.

## FUNDING

This research was funded by the European Union's Horizon 2020 research and innovation programs under the Marie Skłodowska-Curie Grant agreement No. 844703, the European Union's Horizon 2020 research and innovation program under grant agreement No. 730984, ASSEMBLE Plus project (Transnational Access #11154) and the FCT - Foundation for Science and Technology through Stimulus of Scientific Employment, Individual Support (CEECIND; 3rd Edition 2020.01282.CEECIND). This study was also supported by the Portuguese national funds from FCT - Foundation for Science and Technology through projects UIDB/04326/2020, UIDP/04326/2020 and LA/P/0101/2020, and from the operational programs CRESCE Algarve 2020 and COMPETE 2020 through project EMBRC.PT ALG-01-0145-FEDER-022121. PH was supported by grants from FINEP/Rede CLIMA (01.13.0353-00) and CNPq-Universal (426215/2016-8). VS was supported by the scholarship CNPq PIBIC 135940/2016-8. CR and PN were financially supported by the Oceanic Observatory of Madeira Project (M1420- 01-0145-FEDER-000001 - Observatório Oceânico da Madeira-OOM).

## ACKNOWLEDGMENTS

NS thanks intern Marie Brock for her help with the alkalinity sample analysis, Maeve Edwards (National University of Galwey) for her support with the experiments in Ireland, and Miguel Rodrigues (DiveSpot) and the AguaViva team for their support with the fieldwork at Armação de Pêra (Portugal) and in Arvoredo (Brazil), respectively. The authors thank the Museu da Baleia da Madeira for the logistical support during the sampling efforts in Caniçal, the Instituto das Florestas e Conservação da Natureza for house assistance in Porto Santo Island, and Estação de Biologia Marinha do Funchal for all the logistical support during the Madeira Island field campaigns. In Canary Islands, rhodolith samples were collected under license n° SGPM/BDM/AUTSPP/5212019, provided by the General Sub-Directorate General for the Protection of the Sea (Ministry for the

Ecological Transition and the Demographic Challenge- Spain). VP thanks Marie Marbaix (Museum national d'Histoire Naturelle) for their help with molecular work. Acquisition of part of the molecular data was carried out at the 'Service de Systématique Moléculaire', UMS 2700 2AD, MNHN, CNR. The authors are also thankful for the thorough revision and helpful comments by reviewers, which greatly improved the quality of the manuscript.

## SUPPLEMENTARY MATERIAL

The Supplementary Material for this article can be found online at: <https://www.frontiersin.org/articles/10.3389/fmars.2022.921639/full#supplementary-material>

## REFERENCES

- Adams, L. A., Maneveldt, G. W., Green, A., Karenzi, N., Parker, D., Samaai, T., et al. (2020). Rhodolith Bed Discovered Off the South African Coast. *Diversity* 12, 125. doi: 10.3390/d12040125
- Adey, W. H., Halfar, J., and Williams, B. (2013). The Coralline Genus *Clathromorphum* Foslie Emend. Adey: Biological, Physiological, and Ecological Factors Controlling Carbonate Production in an Arctic-Subarctic Climate Archive. *Smithsonian Contr. Mar.Sci.* 40, 1–41.
- Allemand, D., and Grillo, M. C. (1992). Biocalcification Mechanism in Gorgonians: <sup>45</sup>Ca Uptake and Deposition by the Mediterranean Red Coral *Corallium Rubrum*. *J. Exp. Zool.* 262 (3), 237–246. doi: 10.1002/jez.1402620302
- Attard, K. M., Stahl, H., Kamenos, N. A., Turner, G., Burdett, H. L., and Glud, R. N. (2015). Benthic Oxygen Exchange in a Live Coralline Algal Bed and an Adjacent Sandy Habitat: An Eddy Covariance Study. *Mar. Ecol. Prog. Ser.* 535, 99–115. doi: 10.3354/meps11413
- Axelsson, L., Ryberg, H., and Beer, S. (1995). Two Modes of Bicarbonate Utilization in the Marine Green Macroalga *Ulva Lactuca*. *Plant Cell Environ.* 18, 439–445. doi: 10.1111/j.1365-3040.1995.tb00378.x
- Beardall, J., and Giordani, M. (2002). Ecological Implications of Microalgal and Cyanobacterial CO<sub>2</sub> Concentrating Mechanisms, and Their Regulation. *Funct. Plant Biol.* 29, 335–347. doi: 10.1071/PP01195
- Beardall, J., Johnston, A., and Raven, J. (1998). Environmental Regulation of CO<sub>2</sub>-Concentrating Mechanisms in Microalgae. *Can. J. Bot.* 76, 1010–1017. doi: 10.1139/b98-079
- Beck, M. W. (2017). *ggord: ordination plots with ggplot2. R package version 1.0.0.*
- Bergstrom, E., Ordoñez, A., Ho, M., Hurd, C. L., Fry, B., and Diaz-Pulido, G. (2020). Inorganic Carbon Uptake Strategies in Coralline Algae: Plasticity Across Evolutionary Lineages Under Ocean Acidification and Warming. *Mar. Environ. Res.* 161, 105107. doi: 10.1016/j.marenvres.2020.105107
- Berman-Frank, I., Erez, J., and Kaplan, A. (1998). Changes in Inorganic Carbon Uptake During the Progression of a Dinoflagellate Bloom in a Lake Ecosystem. *Can. J. Bot.* 76 (6), 1043–1051. doi: 10.1139/b98-075
- Berman-Frank, I., Kaplan, A., Zohary, T., and Dubinsky, Z. (1995). Carbonic Anhydrase Activity in the Bloom-Forming Dinoflagellate *Peridinium Gatunense*. *J. Phycol.* 31 (6), 906–913. doi: 10.1111/j.0022-3646.1995.00906.x
- Borowitzka, M. A. (1981). Photosynthesis and Calcification in the Articulated Coralline Red Algae *Amphiroa anceps* and *A. foliacea*. *Mar. Biol.* 62, 17–23. doi: 10.1007/BF00396947
- Borowitzka, M. A. (1987). Calcification in Algae: Mechanisms and the Role of Metabolism. *CRC Crit. Rev. Plant Sci.* 6, 1–45. doi: 10.1080/07352688709382246
- Bracchi, V. A., Angeletti, L., Marchese, F., Taviani, M., Cardone, F., Hajdas, I., et al. (2019). A Resilient Deep-Water Rhodolith Bed Off the Egadi Archipelago (Mediterranean Sea) and its Actinopteronological Significance. *Alp. Medit. Quat.* 32 (2), 131–150. doi: 10.26382/AMQ.2019.09
- Bradshaw, A. L., Brewer, P. G., Sharer, D. K., and Williams, R. T. (1981). Measurements of Total Carbon Dioxide and Alkalinity by Potentiometric Titration in the GEOSECS Program. *Earth Planet. Sci. Lett.* 55, 99–115. doi: 10.1016/0012-821X(81)90090-X
- Büdenbender, J., Riebesell, U., and Form, A. (2011). Calcification of the Arctic Coralline Red Algae *Lithothamnion Glaciale* in Response to Elevated CO<sub>2</sub>. *Mar. Ecol. Prog. Ser.* 441, 79–87. doi: 10.3354/meps09405
- Burdett, H. L., Perna, G., McKay, L., Broomhead, G., and Kamenos, N. A. (2018). Community-Level Sensitivity of a Calcifying Ecosystem to Acute *in Situ* CO<sub>2</sub> Enrichment. *Mar. Ecol. Prog. Ser.* 587, 73–80. doi: 10.3354/meps12421
- Carro, B., Lopez, L., Peña, V., Bárbara, I., and Barreiro, R. (2014). DNA Barcoding Allows the Accurate Assessment of European Maerl Diversity: A Proof-Of-Concept Study. *Phyotaxa* 190 (1), 176–189. doi: 10.11646/phytotaxa.190.1.12
- Carvalho, V. F., Assis, J., Serrão, E. A., Nunes, J. M., Batista, A. A., Batista, M. B., et al. (2020). Environmental Drivers of Rhodolith Beds and Epiphytes Community Along the South Western Atlantic Coast. *Mar. Environ. Res.* 154, 104827. doi: 10.1016/j.marenvres.2019.104827
- Chisholm, J. R. W. (2000). Calcification by Crustose Algae on the Northern Great Barrier Reef, Australia. *Limnol. Oceanogr.* 45, 1476–1484. doi: 10.4319/lo.2000.45.7.1476
- Chisholm, J. R. W. (2003). Primary Productivity of Reef-Building Crustose Coralline Algae. *Limnol. Oceanogr.* 48, 1376–1387. doi: 10.4319/lo.2003.48.4.1376
- Comeau, S., Carpenter, R. C., and Edmunds, P. J. (2013). Coral Reef Calcifiers Buffer Their Response to Ocean Acidification Using Both Bicarbonate and Carbonate. *Proc. R. Soc London Ser. B* 280 (1753), 20122374. doi: 10.1098/rspb.2012.2374
- Comeau, S., Cornwall, C. E., DeCarlo, T. M., Doo, S. S., Carpenter, R. C., and McCulloch, M. T. (2019b). Resistance to Ocean Acidification in Coral Reef Taxa is Not Gained by Acclimatization. *Nat. Climate Change* 9, 477–483. doi: 10.1038/s41558-019-0486-9
- Comeau, S., Cornwall, C. E., DeCarlo, T. M., Krieger, E., and McCulloch, M. T. (2018). Similar Controls on Calcification Under Ocean Acidification Across Unrelated Coral Reef Taxa. *Global Change Biol.* 24, 4857–4868. doi: 10.1111/gcb.14379
- Comeau, S., Cornwall, C. E., Pupier, C. A., DeCarlo, T. M., Alessi, C., Trehern, R., et al. (2019a). Flow-Driven Micro-Scale pH Variability Affects the Physiology of Corals and Coralline Algae Under Ocean Acidification. *Sci. Rep.* 9, 12829. doi: 10.1038/s41598-019-49044-w
- Cornwall, C. E., Boyd, P. W., McGraw, C. M., Hepburn, C. D., Pilditch, C. A., Morris, J. N., et al. (2014). Diffusion Boundary Layers Ameliorate the Negative Effects of Ocean Acidification on the Temperate Coralline Macroalga *Arthrocardia corymbosa*. *PLoS One* 9, e97235. doi: 10.1371/journal.pone.0097235
- Cornwall, C. E., Comeau, S., DeCarlo, T. M., Moore, B., D'alexis, Q., and McCulloch, M. T. (2018). Resistance of Corals and Coralline Algae to Ocean

- Acidification: Physiological Control of Calcification Under Natural pH Variability. *Proc. R. Soc B* 285 (1884), 20181168. doi: 10.1098/rspb.2018.1168
- Cornwall, C. E., Comeau, S., and McCulloch, M. T. (2017). Coralline Algae Elevate pH at the Site of Calcification Under Ocean Acidification. *Global Change Biol.* 23, 4245–4256.
- Cornwall, C. E., Hepburn, C. D., Pilditch, C. A., and Hurd, C. L. (2013). Concentration Boundary Layers Around Complex Assemblages of Macroalgae: Implications for the Effects of Ocean Acidification on Understory Coralline Algae. *Limnol. Oceanogr.* 58, 121–130. doi: 10.4319/lo.2013.58.1.0121
- Cornwall, C. E., Revill, A. T., and Hurd, C. L. (2015). High Prevalence of Diffusive Uptake of CO<sub>2</sub> by Macroalgae in a Temperate Subtidal Ecosystem. *Photosynth. Res.* 124 (2), 181–190. doi: 10.1007/s11220-015-0114-0
- de Beer, D., and Larkum, A. (2001). Photosynthesis and Calcification in the Calcifying Algae *Halimeda Discoidea* Studied With Microsensors. *Plant Cell Environ.* 24, 1209–1217. doi: 10.1046/j.1365-3040.2001.00772.x
- Diaz-Pulido, G., Cornwall, C. E., Gartrell, P., Hurd, C. L., and Tran, D. V. (2016). Strategies of Dissolved Inorganic Carbon Use in Macroalgae Across a Gradient of Terrestrial Influence: Implications for the Great Barrier Reef in the Context of Ocean Acidification. *Coral Reefs* 35, 1327–1341. doi: 10.1007/s00338-016-1481-5
- Digby, P. S. B. (1977). Photosynthesis and Respiration in the Coralline Algae, *Clathromorphum Circumscriptum* and *Corallina officinalis* and the Metabolic Basis of Calcification. *J. Mar. Biol. Ass. U.K.* 57, 1111–1124. doi: 10.1017/S0025315400026163
- Drechsler, Z., and Beer, S. (1991). Utilization of Inorganic Carbon by *Ulva Lactuca*. *Plant Physiol.* 97, 1439–1444. doi: 10.1104/pp.97.4.1439
- Dubois, P., and Chen, C. P. (1989). Calcification in Echinoderms. *Echinoderm Stud.* 3, 109–178.
- Farias, J. N., Riosmena-Rodríguez, R., Bouzon, Z., Oliveira, E. C., and Horta, P. A. (2010). *Lithothamnion Superpositum* (Corallinales; Rhodophyta): First Description for the Western Atlantic or Rediscovery of a Species? *Phycol. Res.* 58, 210–216. doi: 10.1111/j.1440-1835.2010.00581.x
- Figueiredo, M. A. O., Coutinho, R., Villas-Boas, A. B., Tâmega, F. T. S., and Mariath, R. (2012). Deep-Water Rhodolith Productivity and Growth in the Southeastern Atlantic. *J. Appl. Ecol.* 24, 487–493. doi: 10.1007/s10811-012-9802-8
- Foster, M. S. (2001). Rhodoliths: Between Rocks and Soft Places. *J. Phycol.* 37 (5), 659–667. doi: 10.1046/j.1529-8817.2001.00195.x
- Fragkopoulou, E., Serrão, E. A., Horta, P. A., Koerich, G., and Assis, J. (2021). Bottom Trawling Threatens Future Climate Refugia of Rhodoliths Globally. *Front. Mar. Sci.* 7. doi: 10.3389/fmars.2020.594537
- Giordano, M., Beardall, J., and Raven, J. A. (2005). CO<sub>2</sub> concentrating mechanisms in algae: mechanisms, environmental modulation, and evolution. *Ann. Rev. Plant Biol.* 56(1), 99–131. doi: 10.1146/annurev.arplant.56.032604.144052
- Gouy, M., Guindon, S., and Gascuel, O. (2010). SeaView Version 4: A Multiplatform Graphical User Interface for Sequence Alignment and Phylogenetic Tree Building. *Mol. Biol. Evol.* 27, 221–224. doi: 10.1093/molbev/msp259
- Hansson, I., and Jagner, D. (1973). Evaluation of the Accuracy of Gran Plots by Means of Computer Calculations: Application to the Potentiometric Titration of the Total Alkalinity and Carbonate Content in Sea Water. *Anal. Chim. Acta* 75, 363–373. doi: 10.1016/S0003-2670(01)82503-4
- Harvey, A. S., Harvey, R. M., and Merton, E. (2017). The Distribution, Significance and Vulnerability of Australian Rhodolith Beds: A Review. *Mar. Freshw. Res.* 68, 411–428. doi: 10.1071/MF15434
- Hofmann, L. C., and Heesch, S. (2018). Latitudinal Trends in Stable Isotope Signatures and Carbon-Concentrating Mechanisms of Northeast Atlantic Rhodoliths. *Biogeosciences* 15, 6139–6149. doi: 10.5194/bg-15-6139-2018
- Hofmann, L. C., Koch, M., and de Beer, D. (2016). Biotic Control of Surface pH and Evidence of Light-Induced H<sup>+</sup> Pumping and Ca<sup>2+</sup>-H<sup>+</sup> Exchange in a Tropical Crustose Coralline Alga. *PLoS One* 11, e0159057. doi: 10.1371/journal.pone.0159057
- Hofmann, L. C., Schoenrock, K. M., and de Beer, D. (2018). Arctic Coralline Algae Elevate Surface pH Annd Carbonate in the Dark. *Front. Plant Sci.* 9. doi: 10.3389/fpls.2018.01416
- Hunter, J. D. (2007). Matplotlib: A 2D Graphics Environment. *Computing Sci. Eng.* 9 (03), 90–95.
- Hurd, C. L., Cornwall, C. E., Currie, K. I., Hepburn, C. D., McGraw, C. M., Hunter, K. A., et al. (2011). Metabolically Induced pH Fluctuations by Some Coastal Calcifiers Exceed Projected 22nd Century Ocean Acidification: A Mechanism for Differential Susceptibility. *Global Change Biol.* 17, 3254–3262. doi: 10.1111/j.1365-2486.2011.02473.x
- Ip, Y. K., Lim, A. L. L., and Lim, R. W. L. (1991). Some Properties of Calcium-Activated Adenosine Triphosphatase From the Hermatypic Coral *Galaxea Fascicularis*. *Mar. Biol.* 111 (2), 191–197. doi: 10.1007/BF01319700
- Jeong, J. B., Kim, S. Y., Seo, Y. K., Kim, J.-K., Shin, J., and Woo, K. S. (2019). Influence of Submarine Topography and Associated Sedimentary Processes on the Distribution of Live and Dead Rhodoliths Near Udo Island, Korea. *Geo-Marine Lett.* 40 (1), 35–51. doi: 10.1007/s00367-019-00623-w
- Johnston, A. M. (1991). The Acquisition of Inorganic Carbon by Marine Macroalgae. *Can. J. Bot.* 69, 1123–1132. doi: 10.1139/b91-144
- Kamenos, N. A., Burdett, H. L., Aloisio, E., Findlay, H. S., Martin, S., Longbone, C., et al. (2013). Coralline Algal Structure is More Sensitive to Rate, Rather Than the Magnitude, of Ocean Acidification. *Global Change Biol.* 19, 3621–3628. doi: 10.1111/gcb.12351
- Kim, J.-H., Steller, D. L., and Edwards, M. S. (2020). Variation in Photosynthetic Performance Relative to Thaluss Microhabitat Heterogeneity in *Lithothamnion Australe* (Rhodophyta, Corallinales) Rhodoliths. *J. Phycol.* 57 (1), 234.244. doi: 10.1111/jpy.13080
- King, R. J., and Schramm, W. (1982). Calcification in the Maerl Coralline Alga *Phymatolithon Calcareum*: Effects of Salinity and Temperature. *Mar. Biol.* 70, 197–204.
- Kingsley, R. J., and Norimitsu, W. (1985). Ca-ATPase Localization and Inhibition in the Gorgonian *Leptogorgia Virgulata* (Lamarck)(Coelenterata: Gorgonacea). *J. Exp. Mar. Biol. Ecol.* 93 (1-2), 157–167. doi: 10.1016/0022-0981(85)90156-X
- Koch, M., Bowes, G., Ross, C., and Zhang, X.-H. (2013). Climate Change and Ocean Acidification Effects on Seagrasses and Marine Macroalgae. *Global Change Biol.* 19, 103–132. doi: 10.1111/j.1365-2486.2012.02791.x
- Legrand, E., Kutti, T., Casal, E. V. G., Rastrick, S. P., Andersen, S., and Husa, V. (2021). Reduced Physiological Performance in a Free-Living Coralline Alga Induced by Salmon Faeces Deposition. *Aquacult. Environ. Interact.* 13, 225–236. doi: 10.3354/aei00403
- Legrand, E., Riera, P., Lutier, M., Coudret, J., Grall, J., and Martin, S. (2017). Species Interactions can Shift the Response of a Maerl Bed Community to Ocean Acidification and Warming. *Biogeosciences* 14, 5359–5376. doi: 10.5194/bg-14-5359-2017
- Legrand, E., Riera, P., Lutier, M., Coudret, J., Grall, J., and Martin, S. (2019). Grazers Increase the Sensitivity of Coralline Algae to Ocean Acidification and Warming. *J. Sea Res.* 148–149, 1–7. doi: 10.1016/j.seares.2019.03.001
- Littler, M. M., Littler, D. S., and Hanisack, M. D. (1991). Deep-Water Rhodolith Distribution, Productivity, and Growth History at Sites of Formation and Subsequent Degradation. *J. Exp. Mar. Biol. Ecol.* 150, 163–182. doi: 10.1016/0022-0981(91)90066-6
- MAArE (2017). *Projeto De Monitoramento Ambiental Da Reserva Biológica Marinha do Arvoredo E Entorno* (Florianópolis, Brazil: ICMBio/UFSC).
- Maberly, S. C. (1990). Exogenous Sources for Inorganic Carbon for Photosynthesis by Marine Macroalgae. *J. Phycol.* 26, 439–449. doi: 10.1111/j.0022-3646.1990.00439.x
- Maberly, S. C., Raven, J. A., and Johnston, A. M. (1992). Discrimination Between <sup>12</sup>C and <sup>13</sup>C by Marine Plants. *Oecologia* 91, 481–492. doi: 10.1007/BF00650320
- Marshall, A. T., and Clode, P. I. (2003). Light-Regulated Ca<sup>2+</sup> Uptake and O<sub>2</sub> Secretion at the Surface of a Scleractinian Coral *Galaxea Fascicularis*. *Comp. Biochem. Physiol. Part A* 136, 417–426. doi: 10.1016/s1095-6433(03)00201-0
- Martin, S., Castets, M. D., and Clavier, J. (2006). Primary Production, Respiration and Calcification of the Temperate Free-Living Coralline Alga *Lithothamnion Corallioides*. *Aquat. Bot.* 85 (2), 121–128. doi: 10.1016/j.aquabot.2006.02.005
- Martin, S., Charnoz, A., and Gattuso, J.-P. (2013). Photosynthesis, Respiration and Calcification in the Mediterranean Crustose Coralline Alga *Lithophyllum Cabiochae* (Corallinales, Rhodophyta). *Eur. J. Phycol.* 48, 163–172. doi: 10.1080/09670262.2013.786790

- Martin, S., Clavier, J., Chauvaud, L., and Thouzeau, G. (2007b). Community Metabolism in Temperate Maerl Beds. II. Nutrient Fluxes. *Mar. Ecol. Prog. Ser.* 335, 31–41. doi: 10.3354/meps335019
- Martin, S., Clavier, J., Chauvaud, L., and Thouzeau, G. (2007a). Community Metabolism in Temperate Maerl Beds. I. Carbon and Carbonate Fluxes. *Mar. Ecol. Prog. Ser.* 335, 19–29. doi: 10.3354/meps335019
- Martin, S., Clavier, J., Guarini, J.-M., Chauvaud, L., Hily, C., Grall, J., et al. (2005). Comparison of *Zostera Marina* and Maerl Community Metabolism. *Aquat. Bot.* 83, 161–174. doi: 10.1016/j.aquabot.2005.06.002
- Martin, S., and Hall-Spencer, J. M. (2017). “Effects of Ocean Warming and Acidification on Rhodolith/Maerl Beds,” in *Rhodolith/maerl Beds: A Global Perspective*. Eds. R. Riosmena-Rodríguez, W. Nelson and J. Aguirre (Berlin: Springer), 55–85. doi: 10.1007/978-3-319-29315-8\_3
- McConnaughey, T. (1989). “Biom mineralization Mechanisms,” in *Origin, Evolution, and Modern Aspects of Biomineralization in Plants and Animals*. Ed. R. E. Crick (New York: Springer), 57–73. doi: 10.1007/978-1-4757-6114-6\_5
- McConnaughey, T. A., and Falk, R. H. (1991). Calcium-Proton Exchange During Algal Calcification. *Biol. Bull.* 180, 185–195. doi: 10.2307/1542440
- McConnaughey, T. A., and Whelan, J. F. (1997). Calcification Generates Protons for Nutrient and Bicarbonate Uptake. *Earth-Science Rev.* 42 (1-2), 95–117. doi: 10.1016/S0012-8252(96)00036-0
- McKinney, W. (2011). Pandas: A Foundational Python Library for Data Analysis and Statistics. *Python High Perform. Sci. computing* 14 (9), 1–9.
- McNicholl, C., Koch, M. S., and Hofmann, L. C. (2019). Photosynthesis and Light-Dependent Proton Pumps Increase Boundary Layer pH in Tropical Macroalgae: A Proposed Mechanism to Sustain Calcification Under Ocean Acidification. *J. Exp. Mar. Biol. Ecol.* 521, 151208. doi: 10.1016/j.jembe.2019.151208
- Mercado, J. M., Carmen, B., Pérez-Lloréns, J. L., and Vergara, J. J. (2009). Carbon Isotopic Fractionation in Macroalgae From Cádiz Bay (Southern Spain): Comparison With Other Bio-Geographic Regions. *Est. Coast. Shelf Sci.* 85 (3), 449–458. doi: 10.1016/j.ecss.2009.09.005
- Mori, I. C., Sato, G., and Okazaki, M. (1996).  $Ca^{2+}$ -Dependent ATPase Associated With Plasma Membrane From a Calcareous Alga, *Serraticardia Maxima* (Corallinaceae, Rhodophyta). *Phycol. Res.* 44, 193–202. doi: 10.1111/j.1440-1835.1996.tb00049.x
- Narvarte, B. C. V., Nelson, W. A., and Roleda, M. Y. (2020). Inorganic Carbon Utilization of Tropical Calcifying Macroalgae and the Impacts of Intensive Mariculture-Derived Coastal Acidification on the Physiological Performance of the Rhodolith. *Sporolithon sp. Environ. Poll.* 266, 115344. doi: 10.1016/j.envpol.2020.115344
- Nash, M. C., Diaz-Pulido, G., Harvey, A. S., and Adey, W. (2019). Coralline Algal Calcification: A Morphological and Process-Based Understanding. *PLoS One* 14 (9), e0221396. doi: 10.1371/journal.pone.0221396
- Neves, P., Silva, J., Peña, V., and Ribeiro, C. (2021). “Pink Round Stones”—Rhodolith Beds: An Overlooked Habitat in Madeira Archipelago. *Biodiv. Conserv.* 30 (12), 3359–3383. doi: 10.1007/s10531-021-02251-2
- Noisette, F., Duong, G., Six, C., Davoult, D., and Martin, S. (2013a). Effects of Elevated  $P_{CO_2}$  on the Metabolism of a Temperate Rhodolith *Lithothamnion Corallioides* Grown Under Different Temperatures. *J. Phycol.* 49, 746–757. doi: 10.1016/j.jembe.2013.07.006
- Noisette, F., Egilsdottir, H., Davoult, D., and Martin, S. (2013b). Physiological Responses of Three Temperate Coralline Algae From Contrasting Habitats to Near-Future Ocean Acidification. *J. Exp. Mar. Biol. Ecol.* 448, 179–187.
- Okazaki, M. (1977). Some Enzymatic Properties of  $Ca^{2+}$ -Dependent Adenosine Triphosphatase From a Calcareous Red Alga, *Serraticardia Maxima* and its Distribution in Marine Algae. *Bot. Mar.* 20, 347–354. doi: 10.1515/botm.1977.20.6.347
- Okazaki, M., Fujii, M., Usuda, Y., and Furuya, K. (1984). Soluble  $Ca^{2+}$ -Activated ATPase and its Possible Role in Calcification of the Coccolithophorid *Cricosphaera Roscoffensis* Var. *Haptonemofera* (Haptophyta) (Studies on the Calcium Carbonate Deposition of Algae V). *Bot. Mar.* 27, 363–369. doi: 10.1515/botm.1984.27.8.363
- Oksanen, J. (2020). *vegan: Community Ecology Package. R package version 2.5-6.2019*
- Otero-Ferrer, F., Cosme, M., Tuya, F., Espino, F., and Haroun, R. (2020). Effect of Depth and Seasonality on the Functioning of Rhodolith Seabeds. *Est. Coast. Shelf Sci.* 235, 106579. doi: 10.1016/j.ecss.2019.106579
- Pardo, C., Lopez, L., Peña, V., Hernández-Kantún, J., Le Gall, L., Bárbara, I., et al. (2014). A Multilocus Species Delimitation Reveals a Striking Number of Species of Coralline Algae Forming Maerl in the OSPAR Maritime Area. *PLoS One* 9 (8), e104073. doi: 10.1371/journal.pone.0104073
- Payri, C. E. (1997). “*Hydrolithon Reinboldii* Rhodolith Distribution, Growth and Carbon Production of a French Polynesian Reef,” in *Proc. 8th Int. Coral Reef Symp.*, Vol. 1. 755–760. (Balboa, Panama: Smithsonian Tropical Research.
- Peña, V., De Clerck, O., Afonso-Carrillo, J., Ballesteros, E., Bárbara, I., Barreiro, R., et al. (2015b). An Integrative Systematic Approach to Species Diversity and Distribution in the Genus *Mesophyllum* (Corallinales, Rhodophyta) in Atlantic and Mediterranean Europe. *Eur. J. Phycol.* 50, 20–36. doi: 10.1080/09670262.2014.981294
- Peña, V., Pardo, C., López, L., Carro, B., Hernandez-Kantun, J., Adey, W. H., et al. (2015a). *Phymatolithon Lusitanicum* Sp. Nov. (Hapalidiales, Rhodophyta): The Third Most Abundant Maerl-Forming Species in the Atlantic Iberian Peninsula. *Cryptogamie Algol.* 36 (4), 429–459. doi: 10.7872/crya/v36.iss4.2015.429
- Pentecost, A. (1978). Calcification and Photosynthesis in *Corallina Officinalis* L. Using the  $^{14}CO_2$  Method. *Br. Phycol. J.* 13, 383–390. doi: 10.1080/00071617800650431
- Qui-Minet, Z. M., Coudret, J., Davoult, D., Grall, J., Mendez-Sandin, M., Cariou, T., et al. (2019). Combined Effects of Global Climate Change and Nutrient Enrichment on the Physiology of Three Temperate Maerl Species. *Ecol. Evol.* 9, 13787–13807. doi: 10.1002/ece3.5802
- Qui-Minet, Z. N., Davoult, D., Grall, J., Delaunay, C., Six, C., Cariou, T., et al. (2021). Physiology of Maerl Algae: Comparison of Inter- and Intraspecific Variations. *J. Phycol.* 57 (3), 831–848. doi: 10.1111/jpy.13119
- Ratnasingham, S., and Hebert, P. D. N. (2007). The Barcode of Life Data System (Www.Barcodinglife.Org). *Mol. Ecol. Notes* 7, 355–364. doi: 10.1111/j.1471-8286.2007.01678
- Rebelo, A. C., Johnson, M. E., Quartau, R., Rasser, M. W., Melo, C. S., Neto, A. I., et al. (2018). Modern Rhodoliths From the Insular Shelf of Pico in the Azores (Northeast Atlantic Ocean). *Est. Coast. Shelf Sci.* 210, 7–17. doi: 10.1016/j.ecss.2018.05.029
- Rebelo, A. C., Johnson, M. E., Rasser, M. W., Silva, L., Melo, C. S., and Ávila, S. P. (2021). Global Biodiversity and Biogeography of Rhodolith-Forming Species. *Front. Biogeography* 13 (1), e50646. doi: 10.21425/F5FBG50646
- Reid, R. J., and Smith, F. A. (1992). Regulation of Calcium Influx in *Chara*: Effects of  $K^+$ , Ph, Metabolic Inhibition, and Calcium Channel Blockers. *Plant Physiol.* 100 (2), 637–643. doi: 10.1104/pp.100.2.637
- Reynier, M. V., Tâmega, F. T. S., Daflon, S. D. A., Santos, M. A. B., Coutinho, R., and Figueiredo, M. A. O. (2015). Long- and Short-Term Effects of Smothering and Burial by Drill Cuttings on Calcareous Algae in a Static-Renewal Test. *Environ. Toxicol. Chem.* 34, 1572–1577. doi: 10.1002/etc.2938
- Ribeiro, C., and Neves, P. (2020). Habitat Mapping of Cabo Girão Marine Park (Madeira Island): A Tool for Conservation and Management. *J. Coast. Conserv.* 24, 22. doi: 10.1007/s11852-019-00724-9
- Riosmena-Rodríguez, R., Nelson, W., and Aguirre, J. (2017). *Rhodolith/maerl Beds: A Global Perspective* (Switzerland: Springer International Publishing). doi: 10.1007/978-3-319-29315-8
- Saunders, G. W. (2005). Applying DNA Barcoding to Red Macroalgae: A Preliminary Appraisal Holds Promise for Future Applications. *Phil. Trans. R. Soc B* 360, 1879–1888. doi: 10.1098/rstb.2005.1719
- Schoenrock, K. M., Bacquet, M., Pearce, D., Rea, B. R., Schofield, J. E., Lea, J., et al. (2018). Influences of Salinity on the Physiology and Distribution of the Arctic Coralline Algae, *Lithothamnion Glaciale* (Corallinales, Rhodophyta). *J. Phycol.* 54, 690–702. doi: 10.1111/jpy.12774
- Schönknecht, G. (2013). Calcium Signals From the Vacuole. *Plants* 2 (4), 589–614. doi: 10.3390/plants2040589
- Schubert, N., Hofmann, L. C., Almeida Saá, A. C., Moreira, A. C., Arenhart, R. G., Fernandes, C. P., et al. (2021a). Calcification in Free-Living Coralline Algae is Strongly Influenced by Morphology: Implications for Susceptibility to Ocean Acidification. *Sci. Rep.* 11, 11232. doi: 10.1038/s41598-021-90632-6
- Schubert, N., Salazar, V. W., Rich, W. A., Vivanco Bercovich, M., Almeida Saá, A. C., Fadigas, S. D., et al. (2019). Rhodolith Primary and Carbonate Production in a Changing Ocean: The Interplay of Warming and Nutrients. *Sci. Total Environ.* 676, 455–468. doi: 10.1016/j.scitotenv.2019.04.280

- Schubert, N., Santos, R., and Silva, J. (2021b). Living in a Fluctuating Environment Increases Tolerance to Marine Heatwaves in the Free-Living Coralline Alga *Phymatolithon Lusitanicum*. *Front. Mar. Sci.* 8. doi: 10.3389/fmars.2021.791422
- Semese, I. S., Beer, S., and Björk, M. (2009). Seagrass Photosynthesis Controls Rates of Calcification and Photosynthesis of Calcareous Macroalgae in a Tropical Seagrass Meadow. *Mar. Ecol. Prog. Ser.* 382, 41–47. doi: 10.3354/MEPS07973
- Simon-Nutbrown, C., Hollingsworth, P. M., Fernandes, T. F., Kamphausen, L., Baxter, J. M., and Burdett, H. L. (2020). Species Distribution Modeling Predicts Significant Declines in Coralline Algae Populations Under Projected Climate Change With Implications for Conservation Policy. *Front. Mar. Sci.* 7. doi: 10.3389/fmars.2020.575825
- Sissini, M. N., Koerich, G., de Barros-Barreto, M. B., Coutinho, L. M., Gomes, F. P., Oliveira, W., et al. (2021). Diversity, Distribution, and Environmental Drivers of Coralline Red Algae: The Major Reef Builders in the Southwestern Atlantic. *Coral Reefs*. doi: 10.1007/s00338-021-02171-1
- Sissini, M. N., Oliveira, M. C., Gabrielson, P. W., Robinson, N. M., Okolodkov, Y. B., Riosmena-Rodríguez, R., et al. (2014). *Mesophyllum Erubescens* (Corallinales, Rhodophyta) - So Many Species in One Epithet. *Phytotaxa* 190, 299–319. doi: 10.11646/phytotaxa.190.1.18
- Sordo, L., Santos, R., Barrote, I., Freitas, C., and Silva, J. (2020). Seasonal Photosynthesis, Respiration and Calcification of a Temperate Maërl Bed in Southern Portugal. *Front. Mar. Sci.* 7. doi: 10.3389/fmars.2020.00136
- Sordo, L., Santos, R., Barrote, I., and Silva, J. (2018). High CO<sub>2</sub> Decreases the Long-Term Resilience of the Free-Living Coralline Algae *Phymatolithon Lusitanicum*. *Ecol. Evol.* 8, 4781–4792. doi: 10.1002/ece3.4020
- Sordo, L., Santos, R., Barrote, I., and Silva, J. (2019). Temperature Amplifies the Effect of High CO<sub>2</sub> on the Photosynthesis, Respiration, and Calcification of the Coralline Algae *Phymatolithon Lusitanicum*. *Ecol. Evol.* 9 (19), 11000–11009. doi: 10.1002/ece3.5560
- Sordo, L., Santos, R., Reis, J., Shulika, A., and Silva, J. (2016). A Direct CO<sub>2</sub> Control System for Ocean Acidification Experiments: Testing Effects on the Coralline Red Algae *Phymatolithon Lusitanicum*. *Peer J.* 4, e2503. doi: 10.7717/peerj.2503
- Sreeraj, C. R., Abhilash, K. R., Deepak Samuel, V., Krishnan, P., Purvaja, R., and Ramesh, R. (2018). Occurrence of Live Rhodolith Bed of *Lithophyllum Kotschyannum* Unger (Corallinales: Lithophylloidea) in Palk Bay: First Record From India. *Curr. Sci.* 114, 1–3. doi: 10.18520/cs%2Fv114%2Fi03%2F445-446
- Steller, D. L., Hernández-Ayón, J. M., Riosmena-Rodríguez, R., and Cabello-Pasini, A. (2007). Effect of Temperature on Photosynthesis, Growth and Calcification Rates of the Free-Living Coralline Alga *Lithophyllum Margaritae*. *Cienc. Mar.* 33 (4), 441–456. doi: 10.7773/cm.v33i4.1255
- Stento, N. A., Ryba, N. G., Kiegle, E. A., and Bisson, M. A. (2000). Turgor Regulation in the Salt-Tolerant Alga *Chara Longifolia*. *Plant Cell Environ.* 23 (6), 629–637. doi: 10.1046/j.1365-3040.2000.00571.x
- Smith, S. V., and Kinsey, D. W. (1996). "Calcification and organic carbon metabolism as indicated by carbon dioxide". In *Coral Reefs: Research Methods, Monographs on Oceanographic Methodology* Vol. 5 eds D. R. Stoddart and R. E. Johannes (Paris:UNESCO), 469–84
- Tambuté, É., Allemand, D., Mueller, E., and Jaubert, J. (1996). A Compartmental Approach to the Mechanism of Calcification in Hermatypic Corals. *J. Exp. Biol.* 199 (5), 1029–1041. doi: 10.1242/jeb.199.5.1029
- Tamura, K., Stecher, G., Peterson, D., Filipski, A., and Kumar, S. (2013). MEGA6: Molecular Evolutionary Genetics Analysis Version 6.0. *Mol. Biol. Evol.* 30, 2725–2729. doi: 10.1093/molbev/mst197
- Tong, T., Li, Q., Jiang, W., Chen, G., Xue, D., Deng, F., et al. (2021). Molecular Evolution of Calcium Signaling and Transport in Plant Adaptation to Abiotic Stress. *Int. J. Mol. Sci.* 22 (22), 12308. doi: 10.3390/ijms222212308
- Triggle, D. J. (2006). L-Type Calcium Channels. *Curr. Pharm. Des.* 12 (4), 443–457. doi: 10.2174/138161206775474503
- Vásquez-Elizondo, R. M., and Enriquez, S. (2016). Coralline Algal Physiology is More Adversely Affected by Elevated Temperature Than Reduced pH. *Sci. Rep.* 6 (1), 19030. doi: 10.1038/srep19030
- Vieira-Pinto, T., Oliveira, M. C., Bouzon, J., Sissini, M., Richards, J. L., Riosmena-Rodríguez, R., et al. (2014). *Lithophyllum* species from Brazilian coast: range extension of *Lithophyllum margaritae* and description of *Lithophyllum atlanticum* sp. nov. *Corallinales, Corallinophycidae, Rhodophyta, Phytotaxa* 190 (1), 355–69. doi: 10.11646/phytotaxa.190.1.21
- Wang, W.-L., and Yeh, H.-W. (2003). δ<sup>13</sup>C Values of Marine Macroalgae From Taiwan. *Bot. Bull. Acad. Sin.* 44, 107–112.
- Ward, D. H., Amundson, C. L., Fitzmorris, P. J., Menning, D. M., Markis, J. A., Sowl, K. M., et al. (2021). Abundance of a Recently Discovered Alaskan Rhodolith Bed in a Shallow, Seagrass-Dominated Lagoon. *Bot. Mar.* 64 (2), 119–127. doi: 10.1515/bot-2020-0072
- Waskom, M., Botvinnik, O., Ostblom, J., Gelbart, M., Lukauskas, S., Hobson, P., et al. (2020). *Mwaskom/Seaborn: V0. 10.1*. doi: 10.5281/zenodo.3767070
- Watson, E. L., Vincenz, F. F., and Davis, P. W. (1971). Ca<sup>2+</sup>-Activated Membrane ATPase: Selective Inhibition by Ruthenium Red. *Biochim. Biophys. Acta* 249, 606–610. doi: 10.1016/0005-2736(71)90140-4
- Yoon, H. S., Hackett, J. D., and Bhattacharya, D. (2002). A Single Origin of the Peridinin- and Fucoxanthin-Containing Plastids in Dinoflagellates Through Tertiary Endosymbiosis. *Proc. Nat. Acad. Sci. U.S.A.* 99, 11724–11729. doi: 10.1073/pnas.172234799
- Zweng, R. C., Koch, M. S., and Bowes, G. (2018). The Role of Irradiance and C-Use Strategies in Tropical Macroalgae Photosynthetic Response to Ocean Acidification. *Sci. Rep.* 8, 9479. doi: 10.1038/s41598-018-27333-0

**Conflict of Interest:** The authors declare that the research was conducted in the absence of any commercial or financial relationships that could be construed as a potential conflict of interest.

**Publisher's Note:** All claims expressed in this article are solely those of the authors and do not necessarily represent those of their affiliated organizations, or those of the publisher, the editors and the reviewers. Any product that may be evaluated in this article, or claim that may be made by its manufacturer, is not guaranteed or endorsed by the publisher.

Copyright © 2022 Schubert, Peña, Salazar, Horta, Neves, Ribeiro, Otero-Ferrer, Tuya, Espino, Schoenrock, Hofmann, Le Gall, Santos and Silva. This is an open-access article distributed under the terms of the Creative Commons Attribution License (CC BY). The use, distribution or reproduction in other forums is permitted, provided the original author(s) and the copyright owner(s) are credited and that the original publication in this journal is cited, in accordance with accepted academic practice. No use, distribution or reproduction is permitted which does not comply with these terms.